Jakob Büttelmann

Spatio-temporal variability in dune plant communities using UAV and multispectral data

UNIVERSIDADE DO ALGARVE

FACULDADE DE CIÊNCIAS E TECNOLOGIA

2022

Jakob Büttelmann

Spatio-temporal variability in dune plant communities using UAV and multispectral data

Master in Marine and Coastal Sciences

Work performed under the supervision of:

Susana Costas
Katerina Kombiadou

UNIVERSIDADE DO ALGARVE
FACULDADE DE CIÊNCIAS E TECNOLOGIA
2022

Spatio-temporal variability in dune plant communities using UAV and multispectral data

Declaration of authorship of the work

I declare to be the author of this work, which is unique and unprecedented. Authors and works consulted are properly cited in the text and are included in the listing of references.

Jakob Büttelmann

19.12.2022

Copyright

Acknowledgements

Herewith I want to thank my supervisors Susana Costas and Katerina Kombiadou for their help and Support over the last year. Also, thanks to my family and Becca Zug who were always supportive at my side. I also I wish to thank the CIMA Department, who supplied the technical support e.g. drone etc. A very big thank you goes also to the PHD applicant Maria Luísa Serrão Bon de Sousa who was flying the drones and did the image pre-processing.

Resumo

O mapeamento da vegetação, através da identificação do tipo e distribuição das comunidades e espécies vegetais, é crucial para analisar a cobertura vegetal e os padrões espaciais. A compreensão das variabilidades espaciais e temporais das plantas dunares em ligação com a morfodinâmica permite uma maior compreensão do dinamismo e evolução dos ambientes costeiros. Tal análise pode contribuir para o desenvolvimento de planos de gestão costeira que ajudam a implementar a biodiversidade costeira e estratégias de protecção. Esta dissertação apresenta uma abordagem para avaliar a utilização de imagens multiespectrais e explorar a variabilidade da vegetação dunar costeira com dados recolhidos à distância por um Veículo Aéreo Não Tripulado (UAV). Foram escolhidas quatro zonas de estudo diferentes na parte oriental da Península de Ancao, distribuídas alongshore, e cobrindo a backhore e a crista das dunas até à base do lee das dunas. Foram utilizados dados de campo e de UAV, em diferentes épocas, nomeadamente ao longo de um período de dois anos. Foi utilizada uma abordagem de classificação em duas etapas, baseada num índice de vegetação de diferença normalizada e num classificador de Floresta Aleatória. Os resultados mostram desempenhos de classificação de alta precisão ao condensar a cobertura do solo em menos classes e também em áreas menos densamente vegetativas. As classificações resultantes foram posteriormente processadas em termos de alterações transfronteiriças e alterações sazonais. Estas técnicas mostram um elevado potencial futuro para avaliar a vegetação das áreas de dunas costeiras e para apoiar a gestão costeira.

Abstract

The mapping of vegetation, by identifying the type and distribution of plant communities and species, is crucial for analysing vegetation coverage and spatial patterns. Understanding dune plant spatial and temporal variabilities in connection with morphodynamics gives further insight in dynamism and evolution of coastal environments. Such analysis can contribute to the development of coastal management plans that helps to implement coastal biodiversity and protection strategies. This dissertation presents an approach to assess the use of multispectral imagery and explore the variability of coastal dune vegetation with remotely sensed data collected by an Unmanned Aerial Vehicle (UAV). Four different study zones were chosen at the eastern part of the Ancao Peninsula, distributed alongshore, and covering the backshore and the dune crest until the base of the dune lee. Field and UAV data were used, in different seasons namely over an extend of two years. A two-step classification approach, based on a normalized difference vegetation index and Random Forest classifier, was used. The Results show high accuracy classification performances when condensing the groundcover into fewer classes and also in less densely vegetated areas. Resulting classifications were further processed in terms of cross-shore changes and seasonal changes. These technics show a high future potential to assess the vegetation of coastal dune areas and to support coastal management.

Table of Contents

Acknowledgements I

Resumo II

Abstract III

Table of Contents IV

Table of figures V

List of tables VI

Motivation 1

1.Objectives 2

2. A review of the state of the art 3

2.1 Coastal dune eco-geomorphology 3

2.2 Remotely sensed dune vegetation characteristics 6

3. Methods 9

3.1 Site description 9

3.2 Data collection 11

3.3 Data processing 12

4.Results 17

5. Discussion 28

6. Conclusion 31

Appendix A 33

References 38

Table of figures

Figure 1: Dune zonation (Carley & Cox, 2017) 4
Figure 2: Compartments of the dune ridge barrier island (modified from Costas et al., 2022) 5
Figure 3: Location of the study area in the Ria Formosa barrier system (upper panel; red rectangle; after Costas et al. (2021)) and the 4 surveyed plots in the study area (bottom) 11
Figure 4: zone 1 in may 2022 17
Figure 5: zone 2 in may 2022 17
Figure 6: zone 3 in may 2022 17
Figure 7: zone 4 in may 2022 17
Figure 8: Averages of the extracted multi-values (x axis: average wavelength of band 1 to 5; y-axis: digital number) of all four zones combined 20
Figure 9: RF Classification results of zone 1 with 4 classes 21
Figure 10: RF Classification results of zone 2 with 6 classes 23
Figure 11: RF Classification results of zone 3 with 3 classes 24
Figure 12: Across-shore variability of landcover class abundance in zone 1 for all campaigns; x axis is in meters. 25
Figure 13: zone 2, corsshore variation over 11 transects and over different seasons and years 26
Figure 14: zone 3, cross-shore variation over 10 transects over different seasons and years 27
Figure 15: zone 4 cross-shore variation over 7 transects over different seasons and years 27
Figure 16: Histogram of January and may in zone 3 for five classes 29
Figure 17: Winter anomalies in Precipitation, humidity and soil moisture in Portugal (Copernicus, 2022) 31
Figure 18: differences in signals 33
Figure 19: similarities in signals 34
Figure 20: grouping of signals 35

List of tables

Table 1: Spectral Indeces 9
Table 2: dates of data collection (fieldtrips) 11
Table 3:plant species or plant groups which were chosen to be classified 15
Table 4: Classification accuracy assessment metrics(Fake, 2019) 15
Table 5: Plants identified in the study plots in the 3 main dune habitats present 18
Table 6: Dune plants and respective functional types 19
Table 7: Confusion matrix of the RF classifier with the four Landcover classes (may 2022) 22
Table 8:Confusion matrix of the RF classifier with the 6 Landcover classes 23
Table 9: Confusion matrix of the RF classifier with the 3 Landcover classes 24
Table 10:accuracy of plots one for the different dates 35
Table 11: Accuracy for plot 2 for the different dates 36
Table 12: Accuracy for plot 3 for the different dates 37

Motivation

The study of the coastal evolution has been always of great importance, considering that 25% of the world's population live within 100km to the coast, below 100m elevation (Zarnetske et al., 2015). Most coastal landscapes evolve through interaction between sediment and vegetation, building the first lines of defence against the oceanic forces (Costas et al., 2020). These coastal features, such as salt marshes and sandy dunes, provide a quantity of ecosystem services beneficial for humans and nature (Laporte-Fauret, 2020). Coastal dune systems act as natural buffers, protecting people and infrastructure from natural hazards. Depending on their morphology (height, width, shape, continuity) and ecological status (functional plant type distribution and abundance), dune systems can reduce the exposure of coastal areas to storm surges, wave action and coastal floods (Renaud et al., 2016). Furthermore, the establishment of pioneer species that lead to the construction of a foredune, reduce landward sand transport and promote the stabilization of the dune system through eco-geomorphic feedbacks (LaporteFauret et al., 2020). They also provide a rich ecosystem for a variety of species (Duran & Moore, 2014). Coastal dunes may form within a variety of environments, also building barrier islands, surrounding lagoon systems or salt marshes. Barrier islands, covering 10-15% of the coastal areas, are characterised by a high dynamism that allows to shift landwards or seawards, depending on internal and external forces (Zhang, 2016; Zinnert et al., 2017).

Despite the fact that coastal sandy dunes have an important value in terms of coastal protection, they face great pressures through anthropogenic actions and climate change. Most importantly, sea-level rise and stronger and/or more frequent storms pose a significant threat, triggering coastal erosion and destruction (Duran & Moore, 2014). In order to mitigate such impacts, many management plans have been proposed, involving beach nourishment, vegetation planting and sand fencing. However, recent works on coastal protection have proposed a different approach, suggesting a beach stabilization by encouraging the dynamism of the environment in order to re-establish dune diversity and mobility (Laporte-Fauret et al., 2020; Seabloom et al., 2013). These conflicting views on intervention measures, combined with the complex interactions controlling dune evolution, increase the uncertainties regarding dune adaptation to climate change. Therefore, it is crucial to monitor the evolution and adaptation of coastal features such as sandy dunes and their eco-geomorphological feedbacks. Thus, it is critical to understand the spatial and temporal distribution of vegetation coverage in relation to morphology changes of dunes. With further insights into the complexity of dune dynamism our understanding in coastal management strategies can improve (Laporte-Fauret et al., 2020).

1.Objectives

The main goal of this work is to contribute to the understanding of the eco-geomorphic feedbacks between the two main components of coastal dunes: geomorphology (topography) and vegetation coverage (plant communities). Investigating how these feedbacks work and which external or internal factors may affect their mechanisms are key to understand adaptation of these coastal features, due to the importance of these feedbacks on the evolution of dune topography (Hesp, 1989; Stallins, 2005; Durán & Moore, 2014). The latter is key in turn to protect hinterland areas from coastal erosion and inundation.

In order to further understand eco-geomorphic feedbacks and their results over time, it is necessary to understand how these two system components (ecology and geomorphology) behave. This work will focus on identifying vegetation coverage and distribution of plant functional types along and across a coastal dune system, aiming to pinpoint spatio-temporal patterns of vegetation distribution and characteristics and to understand the dynamics associated with them.

For that, the distribution (over time and space) and state of the plants within several focus zones (plots), located along the eastern part of the dune of the Ancão Peninsula (western barrier in the Ria Formosa system; S. Portugal) and surveyed during different seasons and over 2 years, will be analysed using remote sensing data, namely multispectral images collected with an Unmanned Autonomous Vehicle (UAV).

In order to reach this aim, the work addresses the following objectives:

1. Identify the dune vegetation by analysing the vegetation coverage on a community and species level
2. Investigate the spatial variability of the dune vegetation alongshore and across-shore in four different plots
3. Determine the temporal variability of dune vegetation on a seasonal and annual basis over two years.

2. A review of the state of the art

2.1 Coastal dune eco-geomorphology

Coastal dunes are highly complex features that result from the interaction of different driving mechanisms. Their formation requires a supply of beach sediment, onshore winds, capable of transporting sand, and suitable topographic and climatic conditions maintained over a long period, which allow accumulation of sand (Pye, 1983; Pye & Tsoar, 2009). Vegetation, when present, has a significant role in dune development, fixation and dune evolution (Houser 2013). When established, dunes offer a rich ecosystem, which varies greatly in spatial and temporal extent. Barrier islands, in particular, host unique dune landscapes, characterized by a complex and dynamic biodiversity, dependent on local morphologies (Zinnert et al., 2017; Stallins, 2005; Durán & Moore, 2014). Dune vegetation and sediment transport are tightly linked, with the former promoting sand accumulation and vertical growth, and the later affecting plant abundance and distribution. Coastal dune eco-geomorphology tries to quantify these biophysical feedbacks, the formation and modification of coastal landscape through sedimentation and vegetation. This feedback between vegetation coverage and sediment transport has a significant role in shaping and positioning dunes. For example, the spatial and temporal sand supply can determine the amount of vegetation coverage. Conversely the vegetation coverage and type influence the shape and amount of sand accumulation (Zarnetske et al., 2015), and thus dune topography. Overall, the evolution of dunes is controlled by a variety of extrinsic and intrinsic factors, such as frequency and magnitude of transporting winds, incident wind direction, beach fetch and sediment supply effects, dune scarping, vegetation types and density, and moisture content (Houser, 2013).

Plant zonations

Coastal dune landscape in temperate zones is characterized by a variety of distinct plant habitats(fig. 1): upper beach, foredune, back dune and stabilized dune (hind dunes). Occupants of these habitats are naturally selected through their special characteristics. Therefore, upper beach and foredunes accommodate plants tolerant to salt spray, strong winds, and sand burial. These communities are mostly permanent due to the unique requirements in these areas. Further innland, at the lee side of the foredune, sand burial tolerant grasses and forbes gradually cover the sand surface with a dense layer of vegetation. Even shrub and tree species can develop over time in these areas (fig.1) (Wiedemann & Pickart, 2008).

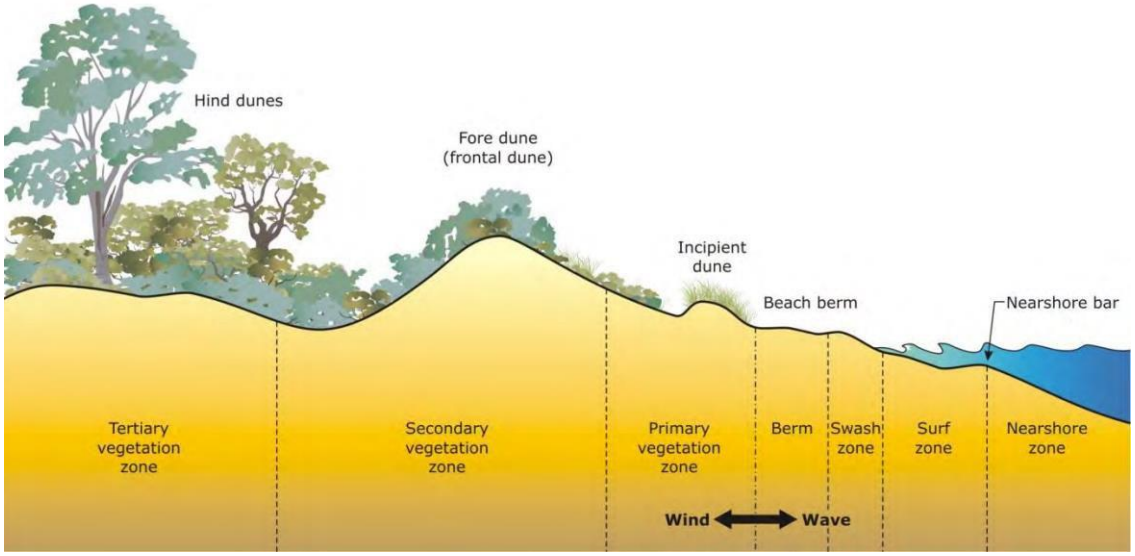

Figure 1: Dune zonation (Carley & Cox, 2017)

Foredunes are defined as shore-parallel dune ridges formed on the top of the backshore by aeolian sand deposition within vegetation (Hesp, 2002). They can be classified into two main types, incipient foredune (embryo dune/incipient dune, new foredune) and established foredune (frontal dune), and represent the first line of vegetation coverage towards the sea (Hesp, 2002). The foredunes and the beach are usually the most critical features on a barrier island. They represent the most essential zones of the coastal barrier system in terms of dynamism and resilience and, due to their dynamic nature, they vary greatly in spatial and temporal extent. Temporal and alongshore variability in dune-beach system adaptation and morphology are mainly controlled by wind regime, wave climate, temperature, precipitation, littoral sediment supply sediment size and mineralogy, and vegetation cover (Houser, 2013).

Plant functional types (PFTs)

From an ecological perspective, especially vegetation type and density are important for the formation and evolution of incipient and established foredunes. Coastal dune plant species can be grouped into nonphylogenetic categories or plant functional types (PFT), depending on their similar responses to environmental conditions and similar effects on the dominant ecosystem processes (Ciccarelli et al., 2009). García-Mora, et al. (1999) distinguish three PFTs in foredunes in the Gulf of Cadiz, categorized in relation to environmental stress and disturbances: Type I, representing mainly winter annuals of moderate size with soft leaves without indication of adaptations to the dune environment. Plants of Type II are mostly perennials with a below ground spreading root network and leaves with presumed adaptations to coastal environmental stress. Type III includes plants mostly capable of being dispersed by seawater and of withstanding sand burial. Type II and type III were found more abundant in unstable soils (incipient fore-

dunes) whereas type I occurs more often in stable soil environment (established foredune). The ratios in occurrence of the three types can be used as an indicator of foredune dynamics (Costas et al. under review).

Vegetation and dune morphology

As mentioned above, the dominant plant type depends on the colonising environment, with growth mainly limited by abiotic factors such as salinity, water stress, substrate instability, sand burial, wind abrasion, high temperature, and low nutrient supply. However, at the same time, plants also contribute to shape their environment (Hesp, 1989; Ciccarelli et al., 2021). In fact, Duran & Moore (2013) argue that vegetation then rather sediment supply is responsible for the maximum dune size. Depending on the plant species, morphology and size, certain foredune morphology is developed (e.g., Zarnetske et al., 2015). For example, in newly formed incipient foredunes, species such as the tall, dense *Ammophila arenaria*, tends to produce higher, more hummocky peaked dune forms than lower, more spreading, rhizomatous plants such as *Spinifex or Ipomoea*, which produce lower, less hummocky dune forms (Davies, 1980; Hesp, 1983, 1984a). This is mainly due to different plant traits and interference with wind flow and sand transport, overall acting as a friction element that slows down the wind, disabling saltation and encouraging sedimentation around the plant (Hesp, 2002). Hesp (1989) distinguishes between four different incipient dune types evolving through these processes: 1, those initiated by shadow dune formation within zones of discrete individual pioneer annuals (e.g. Cakile spp.), and perennials (e.g. Spinifex spp. and *Ammophila* spp.); type 2, those initiated by hummock formation within discrete colonies of perennial grasses and herbs; type 3, those initiated by sand deposition within laterally extensive colonies of pioneer seedlings; and type 4, those initiated by sand deposition within a laterally extensive plant rhizome cover.

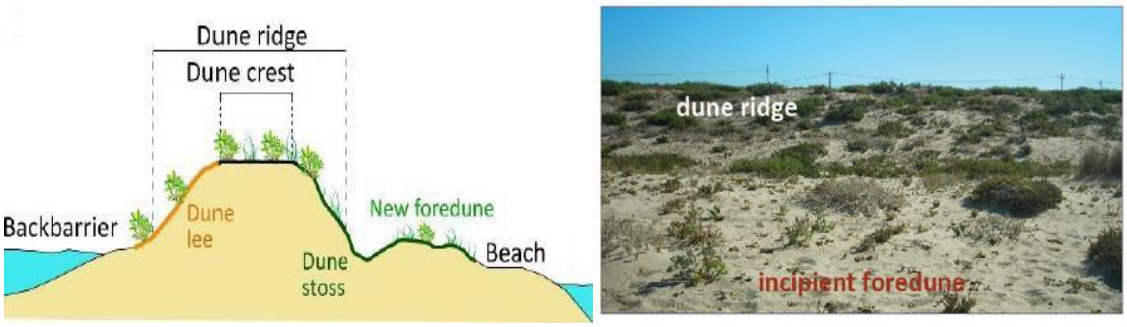

Figure 2: Compartments of the dune ridge barrier island (modified from Costas et al., 2022)

2.2 Remotely sensed dune vegetation characteristics

Dune vegetation mapping and monitoring is crucial to contribute to the understanding of natural and man-made environments, especially in temperate regions, as dune plants are critical for the evolution of the associated landform and it, in turn, adapts to their evolution. Quantifying vegetation cover at different scales and with various techniques gives us further insights in the dynamism and interactions between living organisms and their environment (Xie, Sha, Yu, 2008). Traditional surveys, such as ground-based techniques for measuring and sampling environmental features, have been proven to be successful in studying eco-geomorphology (Maun, 2009; García-Mora, et al., 1999; Acosta et al., 2007). However, these surveys are time consuming, expensive and cover usually small areas. In recent years a rather new approach has been established, using satellite and airborne remote sensing data (Qi, Wang & Zhang, 2013). Remote sensing (RS), the science of obtaining information via noncontact recording, refers to the detection of electromagnetic energy from aircrafts or satellites (Turner et al., 2003). It provides consistent, long-term, Earth observation data at scales from local to global domain. The primary purposes of remote sensing in ecology are to gather land cover and land use information and quantify biophysical variables that connect ecological processes and biodiversity. Next to the traditional field-based surveys, remote sensing has repeatedly proven to be the more efficient method of obtaining ecological data (Lawley et al., 2016; Verbesselt et al., 2010), allowing to cover large areas, consistently monitor changes and survey inaccessible areas (Singh & Frazier, 2018).

Every object can be characterized because of its unique interaction with electromagnetic radiation, which depends on its biophysical properties. For instance, plant size, density and structural composition of branches and leaves define the spectral absorption and reflectance of light for these features. Furthermore, spectral characteristics can be derived from biochemical components, such as chlorophyll, water, proteins, starches, waxes and carbohydrates, giving conclusions about the ecological conditions of vegetation species (Underwood, Ustin, & Ramirez, 2006). Remote sensing utilizes the reflectance spectra of landcover features captured in an image pixel, such as vegetation, soil, and other landcover elements (Turner et al., 2003). The satellite data is limited in spatial resolution (1000-1m), thus can only record on a bigger scale (Kozhoridze et al., 2016). Airborne based applications can get permits to fly on a much lower altitudes, and therefore can provide much higher spatial resolution (<1cm). This is why these

applications are a more reliable approach to identify vegetation communities and complex mosaic landscapes in fine scale and discriminate vegetation at the species level (Adam, Mutanga & Rugege, 2010). In order to reduce costs and time efforts, recent developments mainly focus on multispectral approaches, although, hyperspectral and lidar applications can also be deployed on airborne monitoring systems (Marzialetti et al., 2019).

Unmanned aerial systems (UAS)

Unmanned aerial vehicle, UAV, or the more commonly used term UAS (unmanned aerial system), refers to all kind of 'aerial robots' controlled from the ground. These systems include a variety of drones, which are remotely piloted (Turner, Harley & Drummond, 2016). In recent years, there have been substantial developments in exploring the capabilities of small UASs in relation to ecological research (Anderson et al., 2013; Kaneko et al. 2014; Parjares et al., 2015; McGovern & Gilmer, 2019; Laporte-Fauret, 2020). Their advantages compared to other remote sensing platforms such as satellites, are lower operating heights, which enable the collection of higher spatial resolution images, and the fact that these systems can be deployed quickly, repetitively and independently (Venturi et al., 2016)

An average UAS usually consists of a sensor module for data acquisition, an autopilot for control of the entire aircraft, a GPS (Global Positioning System) for navigation, an IMU (Inertial Measurement Unit) for altitude measurement, and a ground station for controlling and mission planning. The on-board sensors are dependent on the flight mission and purposes. Their range varies from a standard digital camera, multispectral camera, hyperspectral imager and Light Detection and Ranging equipment or LiDAR (Feng, Liu & Gong, 2015). Every sensor has its unique spectral resolution, which determines the boundaries of every monitoring. Navulur (2006) defines five categories of spatial resolution: (i) low or coarse resolution are pixels with ground sampling distance (GSD) of 30m or greater, (ii) medium resolution with GSD in the range of 2.0–30m, (iii) high resolution are pixels with GSD 0.5–2.0m, and (iv) very high resolution refers to pixels sizes <0.5m.

Remotely sensed image classification

As aforementioned, each object features its unique spectral characteristics when penetrated by light. According to their spectral properties, pixels of remotely sensed imagery can be grouped into similar reflectance values and related to a specific landcover. This process is broadly described as image classification and is usually carried out by digital image processing using a variety of different algorithms (Arar et al. 1984; Galio et al. 1985; Suo, McGovern & Gilmer, 2019). When classifying remote sensing imagery many different factors must be considered. The

main steps of image classification include: determination of a suitable classification system, selection of training samples, image pre-processing, feature extraction, selection of suitable classification approaches, post-classification processing, and accuracy assessment (Lu & Weng, 2007).

There are a variety of different strategies for image classification in remote sensing. Most commonly used classification approaches are unsupervised image classification, supervised image classification and object-based image classification. Unsupervised classification is the more traditional and most basic technique since no sampling is needed. It just requires the creation of a cluster and the assignment of classes. It is widely used for mapping thematic vegetation cover from remotely sensed image data (Xie et al., 2008). The main advantages of this strategy, when compared to more advanced techniques (machine learning), come from its relative ease application, as well as its availability in a range of statistical analysis and image processing programs and applications (Langley et al., 2001). Supervised image classification requires the selection of training samples, areas which are key to the accuracy of the method, since they will determine which class each pixel inherits in the image (Ford et al., 2008b). The supervised classification approach is often used for vegetation detection on remote imagery (Suo, McGovern, Gilmer, 2019). Object-based classification groups pixels with relatively homogeneous properties into representative vector shapes with size and geometry. This approach has gained more popularity in recent years because it is useful for high-resolution data (De Giglio et al., 2019).

Using different visible or multispectral data combinations, data processing can help distinguishing vegetation cover. These combinations are known as spectral indices or vegetation indices (VIs), which are often used as a processing step prior to the classification. They are simple but effective algorithms to derive vegetation characteristics, such as growth, vigour, structure and cover (Xue & Su, 2017). For example, the Normalized Differential Vegetation Index (NDVI), which relates the reflectance of land features at near-infrared and red wavebands, is commonly used to distinguish green vegetation areas from other land features, such as water and soil (Gini et al. 2012). A variety of remote sensing studies focused on coastal vegetated properties have successfully incorporated spectral indices (Laporte-Fauret 2020; Marzialetti et al. 2019; Jackson et al. 2019; Proença et al., 2019; Timm & McGarigal, 2012; Corell et al., 2018; Juel et al., 2015**;** Suo, McGovern, Gilmer, 2019). Suo, McGovern & Gilmer, (2019) proposed 6 different spectral indices in connection with multispectral imagery of coastal vegetation cover (Table 1).

Table 1: Spectral Indeces

Spectral Indices	Formula	Explanation
Relative Green	$\frac{\text{Green}}{(Red + Green + Blue)}$	The relative component of green, red and blue bands over the total sum of all camera bands. Less affected from scene illumination conditions than the original band value.
Relative Red	$\frac{Red}{(Red + Green + Blue)}$	
Relative Blue	$\frac{Blue}{(Red + Green + Blue)}$	
Normalized Differential Vegetation Index (NDVI)	$\frac{(NIR - Red)}{(NIR + Red)}$	Relationship between the near-infrared (NIR) and red bands indicates vegetation condition due to chlorophyll absorption within the red spectral range and high reflectance within the NIR range.
gNDVI	$\frac{(NIR + Green)}{(NIR + Green)}$	Improvement of NDVI, accurate in assessing chlorophyll content.
Green-Red Vegetation Index (GRVI)	$\frac{(Green - Red)}{(Green + Red)}$	Relationship between the green and red bands is an effective index for detecting phenophases.

3. Methods

3.1 Site description

The study zones are located at the eastern part of the Ancão Peninsula consisting of 4 separated plots with individual extends of 200 x 200m, in average (Fig. 3). Being part of the Ria Formosa barrier island system, the peninsula provides around 9 kilometers of coastal stretch. The peninsula is urbanised in the center, natural in the western and with small number of houses in the eastern part. The peninsula is limited by the Ancão Inlet on the eastern side (Costas et al., 2020).

The shoreline of the peninsula facing the southwest is primarily shaped by waves coming from W-SW (71%) and E-SE (23%) (Costa et al., 2001), with dominant winds also approaching from WSW (Fig. 3). The mesotidal regime has a mean tidal range of 2.2m with a maximum of 3.5m during spring tides. Net longshore sediment transport in the system is directed eastwards, with

estimates ranging from 6×10^3 up to 3×10^5 m/year (Ferreira et al., 2006). The beach is described as a low tide terrace beach, being reflective during high- and intermediate low tide. Cross-shore the dune morphology and sediment patterns vary significantly. The sediments of the dune beach system consist of medium to coarse quartz sand with mean grain sizes varying from 0.35-0.80mm at the beach and 0.50mm at the dune (Costas et al., 2020).

The oldest aerial pictures of the area, from 1947, show a poorly vegetated dune ridge. Today, herbaceous and shrubby dune species represent the vegetation cover occupying different habitats. Costas et al. (*under review*) refer to three habitat types on the peninsula included in Annex I of the European Habitat Directive 92/43/EEC (2013): (1) Embryo dune, characterized by *Cakile maritima* and *Polygonum maritimum* (habitat type 1210 and 2010), (2) foredune, characterized by the dominance of *Ammophila arenaria*, *Elymus farctus* and *Otanthus maritimus* (habitat type 2120), (3) Fixed coastal dunes with herbaceous vegetation dominated by *Artemisia crithmifolia* and *Lotus creticus* (habitat type 2130). The spatial distribution of vegetation density shows higher values around the crest of the dune ridge with great alongshore variability, with densest vegetation cover found at the very eastern side of the peninsula.

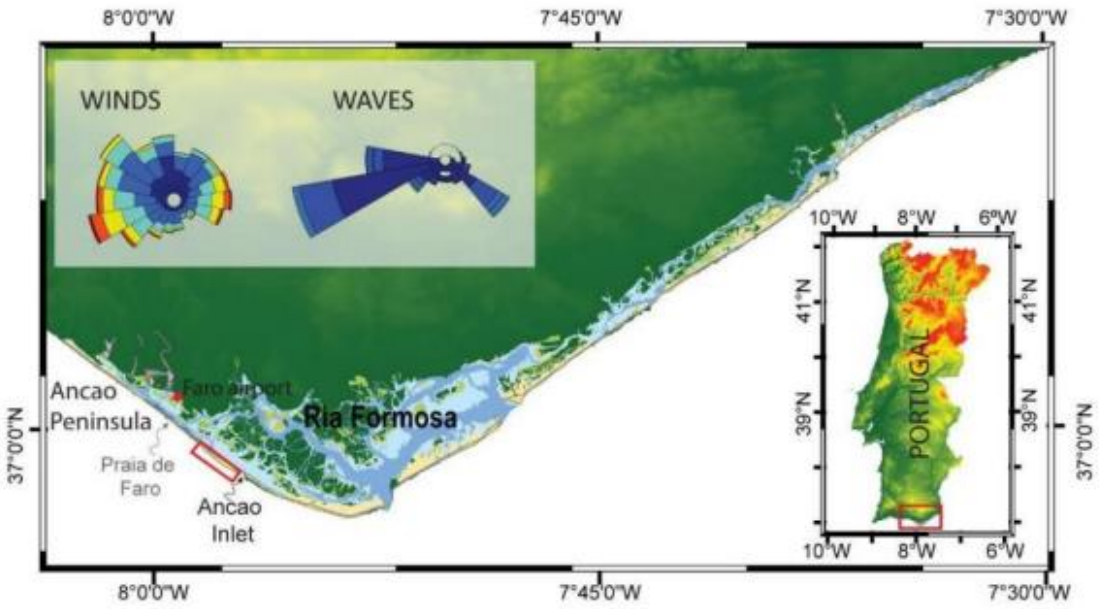

Figure 3: Location of the study area in the Ria Formosa barrier system (upper panel; red rectangle; after Costas et al. (2021)) and the 4 surveyed plots in the study area (bottom)

3.2 Data collection

Airborne multispectral data

Image acquisition was performed using 2 drones, a Phantom 4, equipped with a multispectral camera and a Mavic Pro. Fieldtrips were done in end of January and mid of may, 2022, marked in green (table 2) for all four zones. The data set also includes images that have already been collected in the past two years, marked in blue (table 2). Multispectral images have been taken, using the Phantom 4 Multispectral drone and RGB images have been taken using the Mavic Pro.

Table 2: dates of data collection (fieldtrips)

date	Zone 1	Zone 2	Zone 3	Zone 4
21.05.2020				
26.11.2020				
07.05.2021				
13.10.2021				
31.01/03.02.2022				
18.05.2022				

The acquisition of new images was done in January and May 2022, capturing multispectral data. The image collection with an UAS required the establishment of Ground control points (GCPs) for future improvement of the georeferencing of the collected images. Coordinates of the GCPs were determined using a Trimble Global Navigation Satellite System (GNSS) receiver, connected to the Trimble Virtual Reference Station (VRS). This system can reach 2 cm spatial and 5 cm vertical accuracy for point measurements. The GCPs were later used for georeferencing purposes (Suo, McGovern & Gilmer, 2019).

One of the used drones (Phantom 4 Multispectral from DJI), comprises a 6-band sensor system to record RGB and NIR data with a 4 cm ground resolution. In order to have a better ground resolution and allow plant identification/validation visually, a second drone (Mavic 2 Pro with a three-band (RGB) composition) was used to acquire images with higher resolution (2 cm). The flight height (~30 m) was determined by two factors, firstly the flight permissions due to the proximity to the airport, and secondly by the UAS sensor recording useful imagery to discriminate vegetation on a species level. The flight speed and camera positioning were variable due to weather factors such as wind speed. The error or accuracy of the spatial correction was assessed comparing the product (mosaic or DSM) with check points (independent from the GCPs used for georeferencing) collected during the surveys.

Ground truth data

In order to increase accuracy and define spectral characteristics on a species level, ground measurement data and UAS data are often used in a complementary sense. Coupling both techniques generate more information (Walters & Scholes, 2017). For calibrating and ground-truthing purposes, dune plant species were mapped and identified at different points. The vegetation survey was carried out during the image acquisition of the four zones. For that, a central profile was defined in each site for sampling plant species identification.

3.3 Data processing

The main objective of the processing is to determine the plant communities and species by executing a GIS data analysis of the collected images. This includes the application of a spectral Index, namely the Normalized Different vegetation Index (NDVI) and the choice of the most suitable classification as described below. The analysis was carried out in ArcGIS from Esri software. In order to improve functionality and workflow reproduction of used geoprocessing and image processing tools, the defined workflows have been built on ModelBuilder tool.

Pre-processing

The implementation of a pre-processing step solves the problem of platform sway, sensor displacement, different altitudes, and lightning variations (Feng, Liu, Gong, 2015; Bemis et al., 2014). Pre-processing in this case involved the elaboration of the orthophoto mosaics (both multispectral and RGB)

The images were pre-processed with Agisoft Metashape, a photogrammetric software to produce the orthographic imagery and the associated DSM (digital surface model) out of a point cloud. The GCPs were used to improve georeferencing of the original raw images. The single tiles need to be set together in spatial continuous raster sets to produce the mosaics. The raster creation will be executed by applying a mosaicking process to enhance processing speed and improve image spectral variations.

Spectral signature of the plants

Considering the great amount of different plant species identified within the surveyed plots in the coastal dunes, it was difficult to separate all species with very similar reflectance values in a classification. Therefore, extracting reflectance values in order to assemble a pre-grouping can be helpful. For this, the images were resampled from 0.04m to 0.15m and the raster files were converted to vector files (namely, point shapefiles). In addition, new shapefiles were elaborated that included the mapping of different plant species through visual identification using the RGB images and the ground truth data. The latter included point and polygon shapefiles that included the plant species for each point or polygon.

The shapefiles were intersected for the case of polygon shapefiles in order to obtain the spectral signature (i.e. the digital number of each band) of a specific plant species. In the case of point shapefiles with plant species, the spectral signature was extracted from the raster images. Output tables with the digital number per extracted point and species over the 5 bands were generated for all four zones. Similar species in terms of reflectance were visualized and grouped when possible (see appendix).

Extraction of vegetation cover

Prior to a classification, the vegetation cover was separated from other groundcover features, in order to minimize misclassifications between sand and plants. The Normalized Difference Vegetation Index (NDVI) is a dimensionless index, it varies between -1 and +1, describing the differences between visible and near infrared reflectance. This index is commonly used to measure the amount of photosynthetic biomass and it is mostly applied to separate healthy vegetation from other groundcover features in fine scale environments, such as coastal dunes. (Laporte-Fauret et al., 2020; Verbesselt et al., 2010). It is computed as:

$$NDVI = \frac{(Near - infrared - Red)}{(Near - infrared + Red)}$$

Where Near-infrared and Red refer to the bands withing the spectral range: 700 to 2,500 nm. To discriminate sand from vegetation, a threshold value needs to be established. The most relevant value was chosen by testing different values based on current literature (Laporte-Fauret et al., 2020) and validation tests. The best threshold value was 0.11, which states anything below as non-vegetation cover and anything higher as vegetation cover. The resulting raster just included vegetation cover and were used as classification basis for the classification.

Classification of the vegetation cover

Although the Maximum Likelihood Classification (MLC) is one of the most commonly applied classification techniques for aerial imagery when using pixel or statistical-based distributions (Xie et al., 2008) and has also been used successfully in connection with different coastal studies (De Giglio et al., 2019; Suo, McGovern, Gilmer, 2019), the Random Forest Classifier (RFC) was giving lower errors in the classifications when running the quality test, therefore it has been the preferential choice in this study. RFC has been proven to be a successful tool in detection of coastal vegetation features because of its stability and ability to discriminate fine ground cover differences (Marzialetti et al., 2019; Timm & McGarigal, 2012; Corell et al., 2018; Juel et al. 2015; Laporte-Fauret et al.,2020). This technique is composed of a set of different individual base classifiers (decision trees), each tree giving a decision, and the final decision corresponding to the majority vote (Proença et al., 2019).

The RFC classifier was trained with training classes specific of each zone in order to determinate the spectral signature of each species and/or group (table 3) which were chosen to be classified. After excluding the non-vegetated ground cover with the NDVI index, the resulting raster was used to distinguish the classes by drawing polygons around cells which could be defined as a certain class. Using the GPS location points of the ground truth samples of plant species as reference for the qualitative determination of species. Additionally, the Orthophoto of the Mavic Pro, with a higher resolution were used to define the classes.

The table below (table 3) shows the different species *Artemesia, Eryngium, Otanthus, Calystegia, Paronychia*) and 'Other Plants' which is representative for all other plants used in the classification. Three different classifications in terms of training classes have been tested with two classes, three classes and five classes.

Table 3:plant species or plant groups which were chosen to be classified

classes	*Artemesia campestris* *Other plants*	*Eryngium maritimum* *Othanus* *Other plants*	*Eryngium maritimum* *Calystegia soldanella* *Artemesia campestris* *Paronychia argentea* *Other plants*
Zone 1			
Zone 2			
Zone 3			
Zone 4			

Evaluation of classification performance

Evaluation of classification results is an important step in the classification procedure. Different criteria must be considered, such as classification accuracy, computational resources, stability of the algorithm, and robustness to noise in the training data. However, the accuracy assessment is the most common approach to evaluate the classification performance. After generation of an error matrix, other important accuracy assessment elements, such as overall accuracy, omission error, commission error, and kappa coefficient, can be derived (Lu & Weng, 2007; Jackson et al., 2019).

Table 4: Classification accuracy assessment *metrics (Fake, 2019)*

Accuracy measure	**Equation**	**Result**
Kappa	$\frac{(Observed\ Agreement - Expected\ Agreement}{1 - Expected\ Agreement}$	Difference between the actual agreement and the agreement expected by chance.
Overall Accuracy	$\frac{\text{Number of correct cells}}{\text{total number of cells}}$	The average accuracy of the classification across all cover types. Does not account for error distribution across classes.

Comission	$\frac{\text{Number of incorrect cells in class X}}{\text{Total number of cells classified as class X}}$	Measurement of how much the class has been over-classified
Omission	$\frac{\text{Number of cells in class X that were classified as}}{\text{Total number of cells meant to be in Class X}}$	Measurement of how much the class has been under-classified
Users Accuracy	$\frac{\text{Number of correct cells in class X}}{\text{Number of cells classified as class X}}$	For each class, the probability that a randomly chosen point on the map has the same class value in the field.
Producer Accuracy	$\frac{\text{Number of correct cells in class X}}{\text{Total number of cells meant to be in class X}}$	For each class, the probability that a randomly chosen point in the field has the same value on the map.

To retrieve these Accuracy assessment metrics pointed out above, a reference data need to be used in order to compare with the value after the classification. The assessment was used based on visual determination. The reference data retrieved from the orthophoto mosaic build from the Mavic Pro drone (RGB images with higher spatial resolution). The ground truth pictures and GPS locations have been also used to define ground cover types for the accuracy test. 30 points per class have been created for the accuracy assessment.

Spatial cross-shore variability

To evaluate the cross-shore variability of the vegetation coverage at each plot, from the seaside towards inland of the plot, the plots were divided into up to 11 polygons or sections (depending on the zone). Each section has a width of 10m and a length corresponding to the width of each plot. For each section the plant coverage per plant group/species was calculated in square meters and the density calculated (%). These estimates were only applied to classifications with acceptable accuracy results. Acceptable accuracy results were defined in this work classification results with a Kappa higher than 0.75. The estimate of the changes in the type of vegetation cover was therefore analysed across the dune and over time and compared.

4.Results

Drone imagery

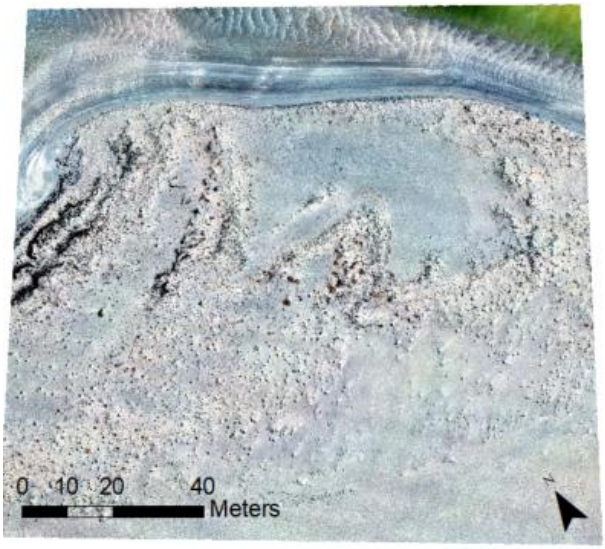

Figure 4: zone 1 in may 2022

Figure 5: zone 2 in may 2022

Figure 6: zone 3 in may 2022

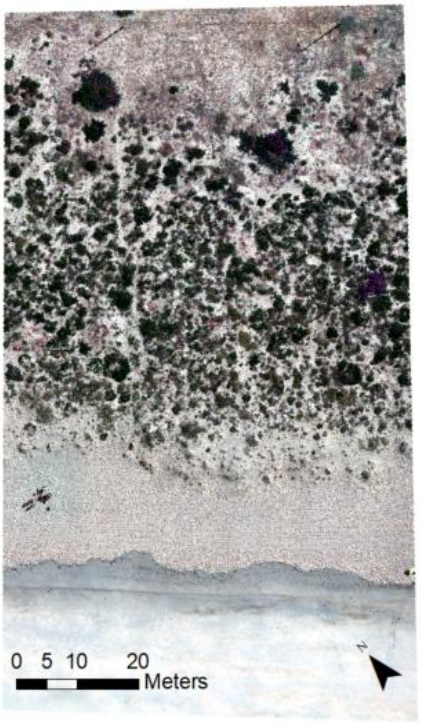

Figure 7: zone 4 in may 2022

The first results in terms of data collection are the pre-processed drone imagery. Zone 2, 3, 4 (fig. 5, 6, 7) seem to have a very similar ground coverage in terms of vegetation cover. The backshore is dominated by bare sand and patchy vegetation cover by very small plants. Moving away from the water, small empty dune formation can be noted with increasing but still scattered vegetation coverage. Whereas the dune ridge can be characterized by isolated, but partly bigger plant patches. Behind the dune ridge, further inland, a significant increase in vegetation coverage can be seen, accompanied by bigger plant patches. Zone 1 (fig. 4) is overall very sparsely vegetated with randomly distributed bigger plan patches, with bare sand being the dominant landcover type.

Plant species

The ground truth sampling resulted in 21 different species detected over all 4 zones. Depending on their location during the fieldtrip the species could be assigned to their coastal habitat Following the Annex I of the European Habitat Directive 92/43/EEC (2013) (table 5). In terms of plant functional types most of the plans could be assigned to the three different types defined by *García Mora et al. (1999)* *(table 6).*

Table 5: Plants identified in the study plots in the 3 main dune habitats present

Embryo dune	**Fordune**	**Established dune**
Eryngium maritinum	*Ammophilia arenaria*	*Artemisia campestris*
Calystegia soldenella	*Pancratium maritinum*	*Paronychia argentea*
Cakile maritima	*Lotus creticus*	*Lotus creticus*
Otanthus maritimus	*Crucianella maritima*	*Anthemis maritima*
Polygonum maritinum	*Otanthus maritimus*	*Aeonium arboreum*
Elymus farctus	*Elymus farcus*	*Carpobrotus acinaciformis*
Pancratium maritinum	*Silene nicaeensis*	*Pelargonium capitatum*
Medicago marina	*Medicagos marina*	*Silene nicaeensis*
Pancratium maritimum	*Linaria pedunculata*	*Malcolmia littorea*
Crucianella maritima	*Euphorbia paralias*	*Ammophila arenaria*
	Malcolmia littorea	
	Artemisia campestris	

Table 6: Dune plants and respective functional types

species	Functional Type (FT)	Burial Tolerant (BT)
Ammophila arenaria	3	TAA
Anthemis maritima	2	NT
Artemisia	2	TBA
Calystegia soldanella	3	TBA
Carpobrotus acinaciformis (invasive)	2	TBA
Crucianella maritima	2	TBA
Elymus farctus	3	TAA
Eryngium maritimum	3	TBA
Linaria pedunculata	2	NT
Lotus criticus	2	TBA
Malcolmia littorea	2	NT
Medicago marina	2	TBA
Otanthus maritimus	3	TAA
Pancratium maritimum	3	TBA
Paronychia argentea	1	NT
Polygonum maritimum	3	TBA
Silene nicaeensis	2	NT

Functional types (FT) according to García Mora et al. (1999), and species burial tolerance (BT): TAA=high burial rates tolerant, TBA=low burial rates tolerant, NT=not tolerant to sand burial.

Spectral signature of plant species

The extraction of multi-values (spectral signature over the 5 bands) averaged over all 4 plots resulted in an output of values for each species for every band (fig. 8) The digital number values are ranging from a minimum of 8441 in band 1 to maximum of 55442 in band 5. Most of the signatures for the species in band 1, 2 and 3 vary in a spectrum of 10.000-30.000, whereas band 4 and band 5 are located in a spectrum between 25.000 and 55.000. There is a strong

mixing between plant species in the dataset, hence the multispectral signal alone cannot be used to separate at the species level the entire vegetation cover.

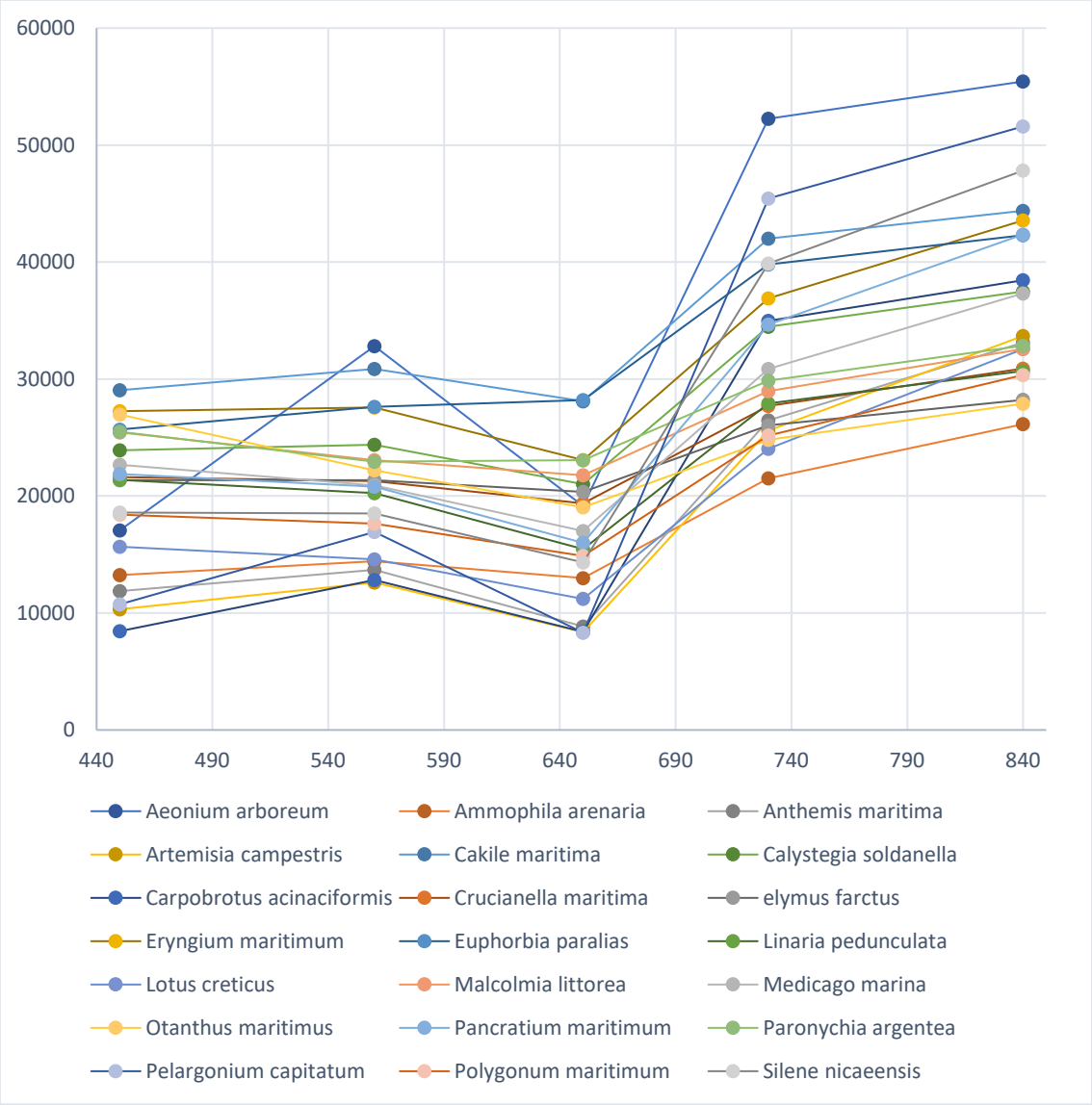

Figure 8: Averages of the extracted multi-values (x axis: average wavelength of band 1 to 5; y-axis: digital number) of all four zones combined

Image Classification

Three vegetation classes were used by the RF classifier for zone 1 after the sand class was extracted through the application NDVI threshold. Two classes were distinguished because of the significant differences in spectral signature of *Eryngium* and *Othantus*. All other species have rather similar signature observing the histogram. The class '*Other*' is therefore a

combination of all other species, which were grouped due to similar signature. The results of the RF classification of May 2022 are given in (fig. 9), as an indicative example, showing that landcover is dominated by sand. The dominant vegetation cover is *Otanthus* and *Other* vegetation. Lowest cover is represented by *Eryngium*. Higher vegetation density is noted towards the lagoon side (north), represented mostly by *Other vegetation* and *Otanthus*, whereas *Eryngium* is more common in the middle and western side. The accuracy test indicates a very good overall accuracy (0.95) and Kappa (0.93) values. The class accuracy of *Otanthus* and Sand have a 100% agreement, whereas *Eryngium* has 93% and other species have 87%, showing very good results as well. Accuracies for all other surveys (table 7; survey date table 2) and all other accuracy values as Comission, Omission, Users accuracy and Producer accuracy see Appendix A.

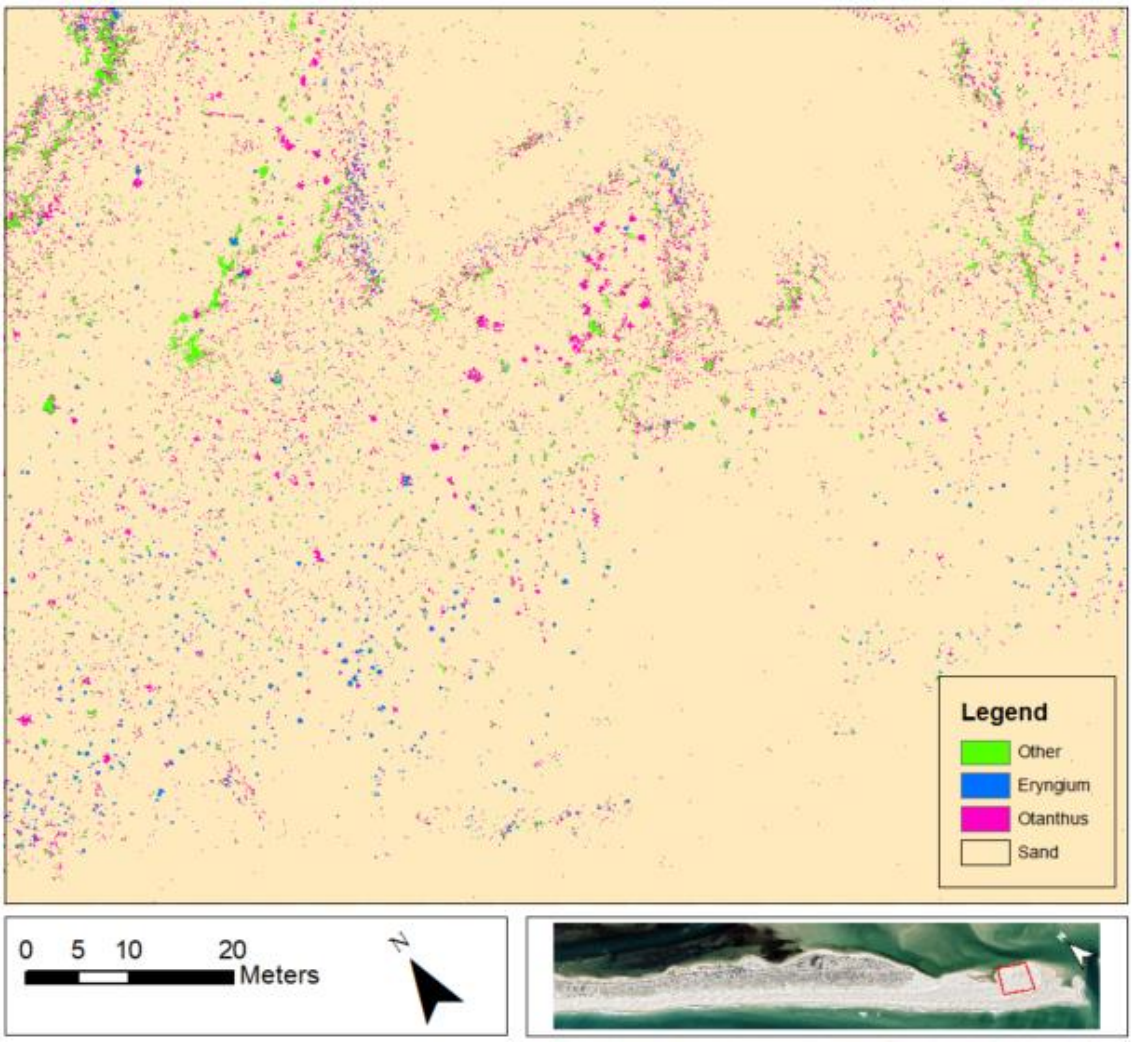

Figure 9: RF Classification results of zone 1 with 4 classes

Table 7: Confusion matrix of the RF classifier with the four Landcover classes (may 2022)

Class	Sand	Otanthus	Eryngium	Other	Class Accuracy (%)
Sand	30	0	0	1	100
Otanthus	0	30	0	1	100
Eryngium	0	0	28	2	93
Other	0	0	2	26	87
Overall accuracy: 0.95					
Kappa: 0.93					

Five vegetation classes were used to classify zone 2 after extraction of the sand class. The results of the RF classification of May 2022 are given in figure 10, as an indicative example, showing dominance of sand class on the backshore beach and embryo dune. Most common plants in the seaward incipient foredune seem to be *Eryngium* and *Calystegia*. Over the landward incipient foredune, vegetation is becoming denser and more dominated by *Other* species and *Artemisia*. The established dune ridge behind the foredune is mainly covered by *Artemisia*, *Paronychia* and sand. The accuracy test shows low overall agreement with an overall accuracy of 0.51 and a Kappa of 0.41. More specifically, class accuracies of sand (80%) and *Artemisia* (86%) show rather good results, but *Eryngium* (43%), *Calystegia* (33%), Other (23%) and *Paronychia* (36%) lower the overall accuracy of the classification. Accuracies for all other campaigns and all other accuracy values as Commission, Omission, Users accuracy and Producer accuracy see Appendix A.

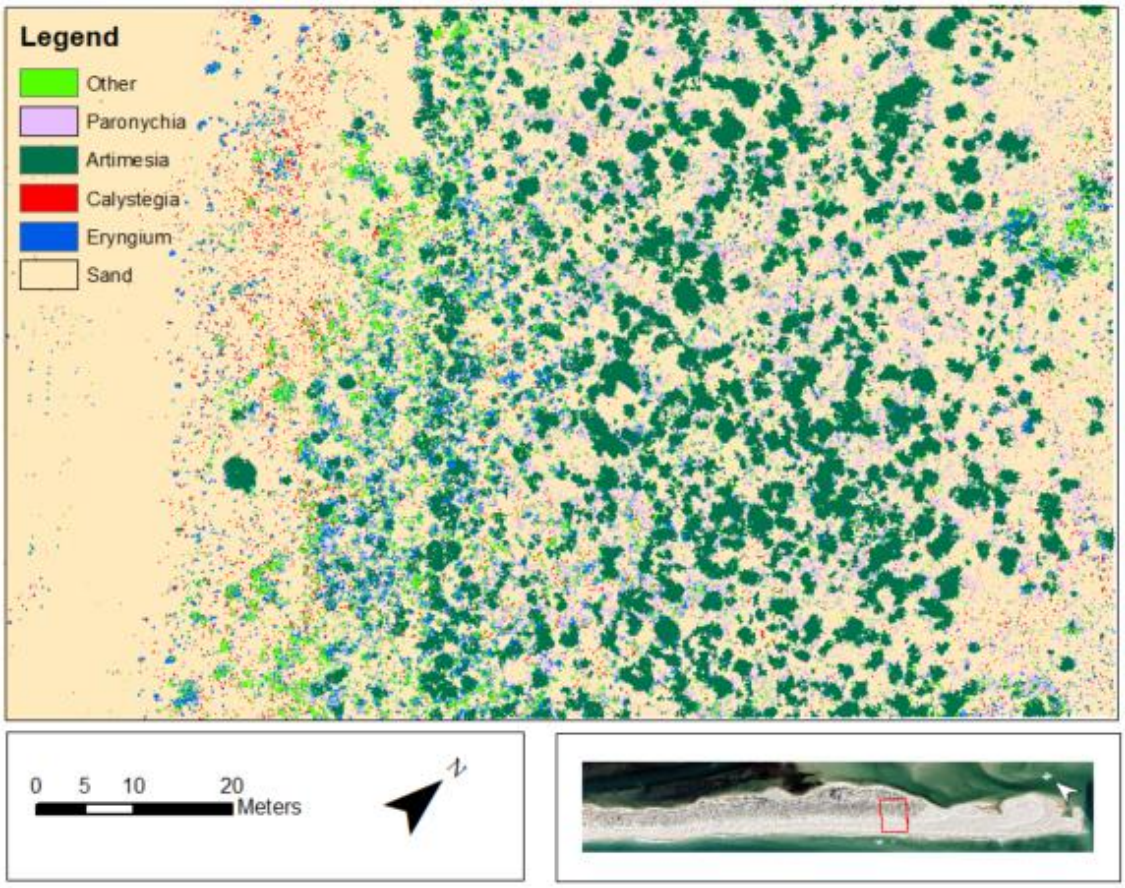

Figure 10: RF Classification results of zone 2 with 6 classes

Table 8:Confusion matrix of the RF classifier with the 6 Landcover classes

Class	Sand	Eryngium	Calystegia	Artemisia	Other	Paronychia	Class Accuracy (%)
Sand	24	5	6	2	4	13	80.00
Eryngium	0	13	2	2	6	0	43.33
Calystegia	2	2	10	0	2	0	33.33
Artemisia	0	0	4	26	5	3	86.67
Other	0	9	7	0	7	3	23.33
Paronychia	4	1	1	0	6	11	36.67
Overall Accuracy: 0.51 Kappa: 0.41							

Two vegetation classes were used to classify zone 3 (after extraction of the sand class). The results of the RF classification of May 2022 are given in figure 11, as an indicative example, showing dominance of sand class on the backshore beach. The incipient foredune is mainly covered by *Other* species and sand, whereas *Artemisia* is dominant over the established dune ridge behind the foredune. The accuracy of the classification is high, with an overall accuracy

of 0.87 and a Kappa of 0.80. Class accuracies for are 93%, 77% and 90% for sand, Other and *Artemisia*, respectively. Accuracies for all other campaigns and all other accuracy values as Commission, Omission, Users accuracy and Producer accuracy see Appendix A.

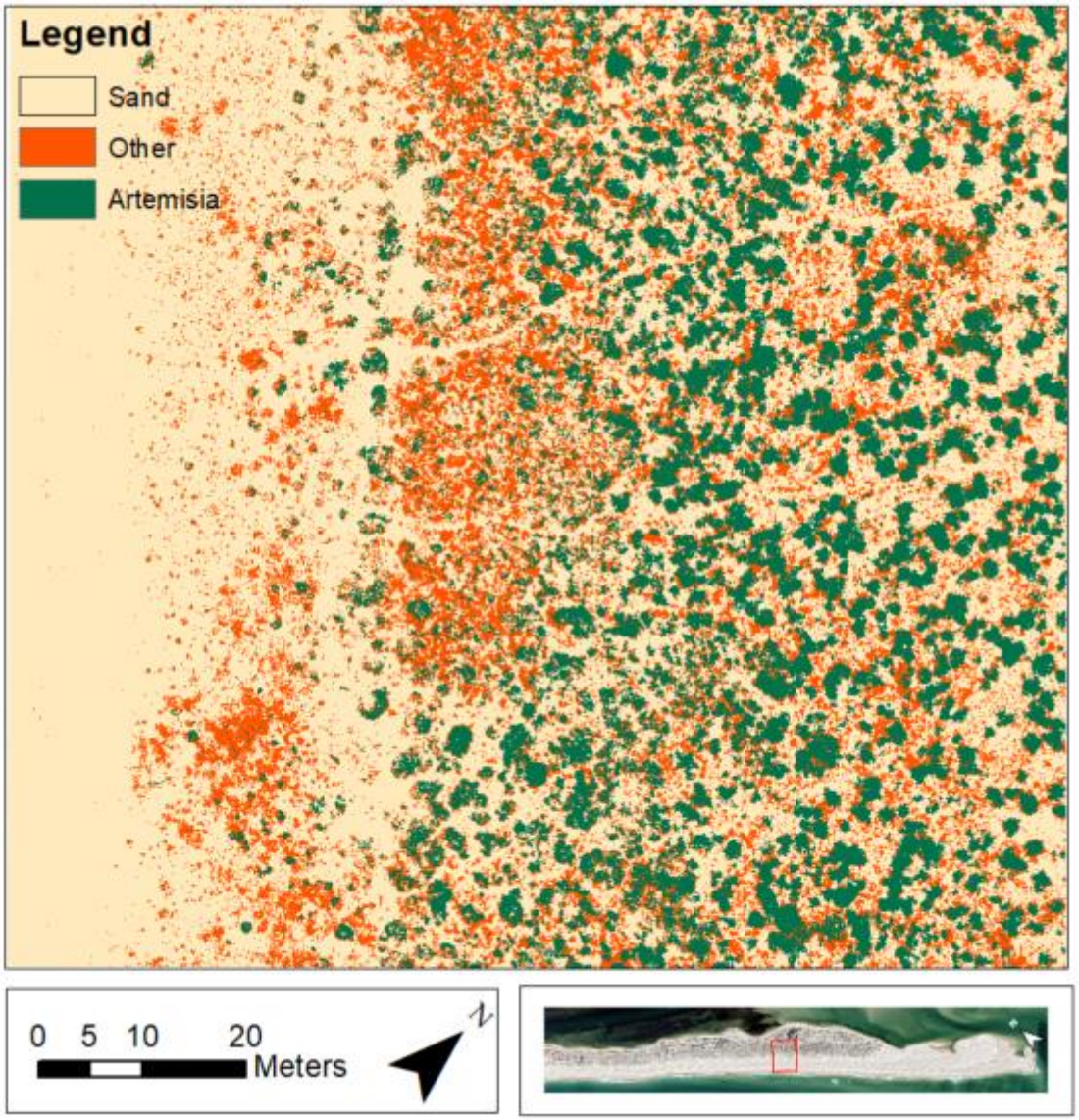

Figure 11: RF Classification results of zone 3 with 3 classes

Table 9: Confusion matrix of the RF classifier with the 3 Landcover classes

Class	Sand	Artemisia	Other	Class accuracy (%)
Sand	28	4	0	93
artemesia	1	23	3	77
other	1	3	27	90
		Overall Accuracy: 0.87		
		Kappa: 0.80		

Spatial and temporal variability of dune landcover

The cross-shore variability in landcover classes over the dune is presented in Figure 12, Figure 13. Figure 14. and Figure 15 for zones 1 to 4, respectively. The vertical axis gives the density of each class, summed over cross-shore sections spaced every 10m (x axis in meters, increasing landwards). Considering the good overall accuracy values from zone 1 with four classes and zone 2 zone 3 and zone 4 with three landcover classes, were the reason to choose these classification for further transect-crosshore evaluation. Zone 2 with 6 classes were excluded because of insufficient accuracy values.

Zone 1 shows a significant opposite cross-shore gradients between sand and vegetation cover, mainly regarding *Otanthus* and *Other* species. *Eryngium* doesn't show a clear pattern, with presence throughout the plot. Over time there an increase of plant species coverage in all 3 classes. The last dataset from May 2022 shows a slight decrease in plant coverage, however this could be within the classification error.

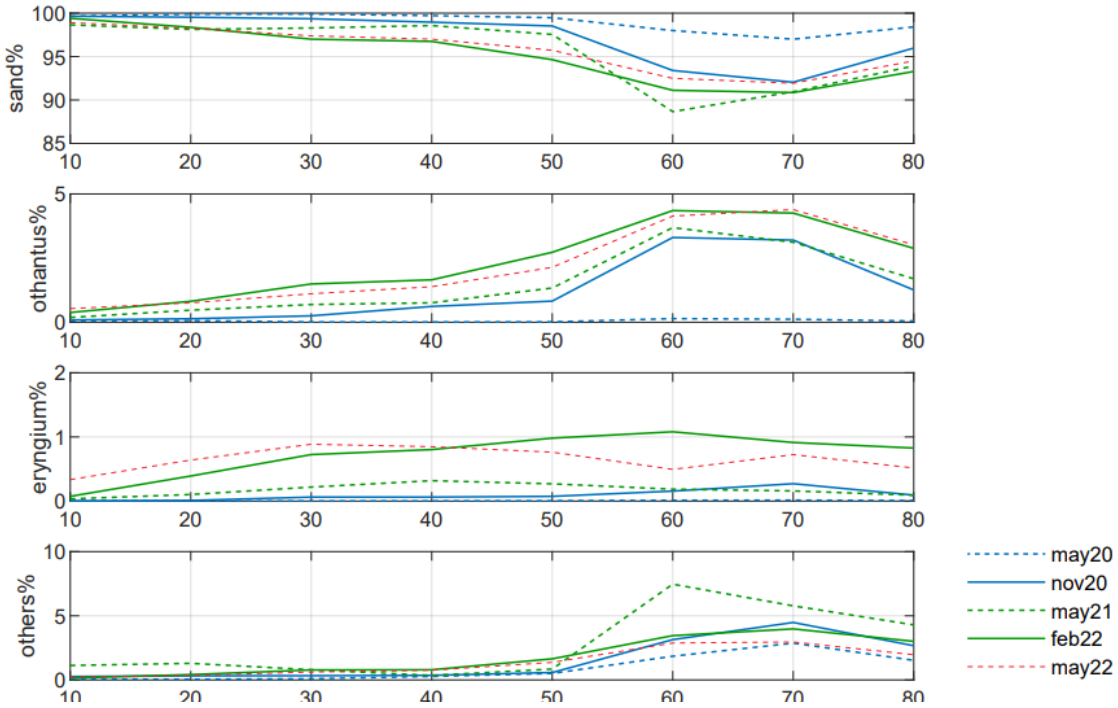

Figure 12: Across-shore variability of landcover class abundance in zone 1 for all campaigns; x axis is in meters.

Zone 2 also shows opposite cross-shore gradients between sand and vegetation cover, for both vegetation classes (*Others* and *Artemisia*, increasing landwards). In the last two sections, a decrease in *Artemisia* and an increase in sand coverage can be observed. Over time, the highest overall sand cover can be observed in May 2020 and the lowest overall sand cover in May 2021. Other species show high variability, with overall increase with time, whereas *Artemisia* shows low interannual variability mainly varying seasonally.

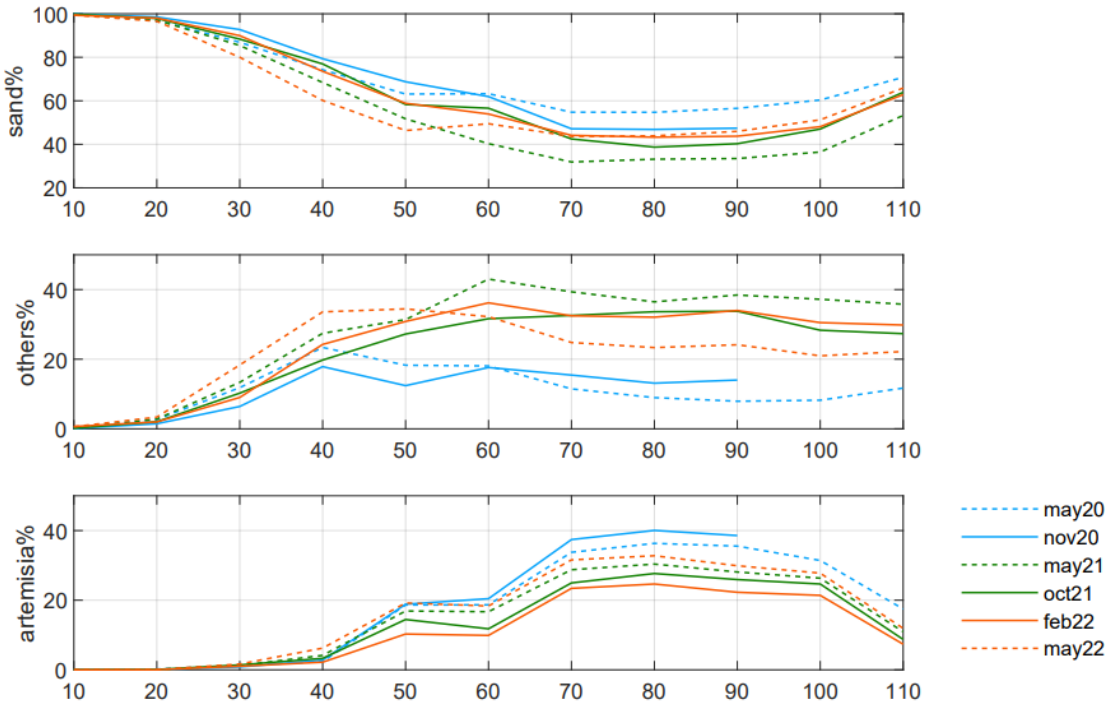

Figure 13: zone 2, corsshore variation over 11 transects and over different seasons and years

Cross-shore gradients in Zone 3 shows the same variability as the other zones, with decreasing trends for sand and increasing ones for *Artemisia*. With and high sand coverage (100%) on the seaside a steady decline over the first 70 meters to under 50% can be observed. Conversely Artemisia start with 0% at the seaside and shows a rapid growth in coverage starting from 30m meters land inwards

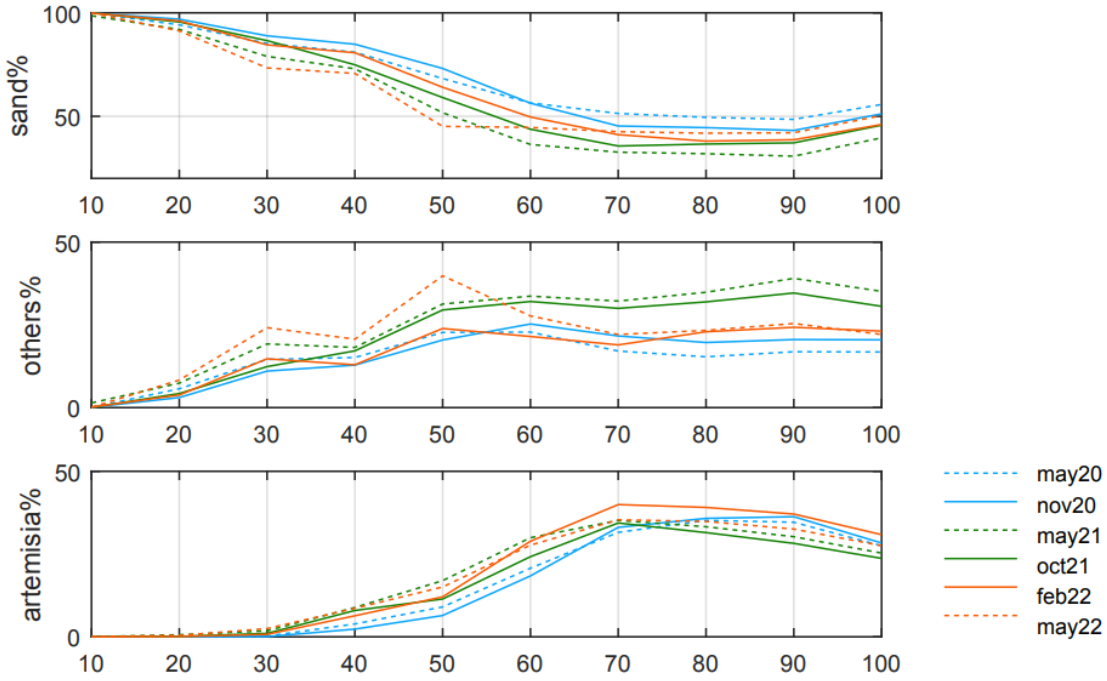

Figure 14: zone 3, cross-shore variation over 10 transects over different seasons and years

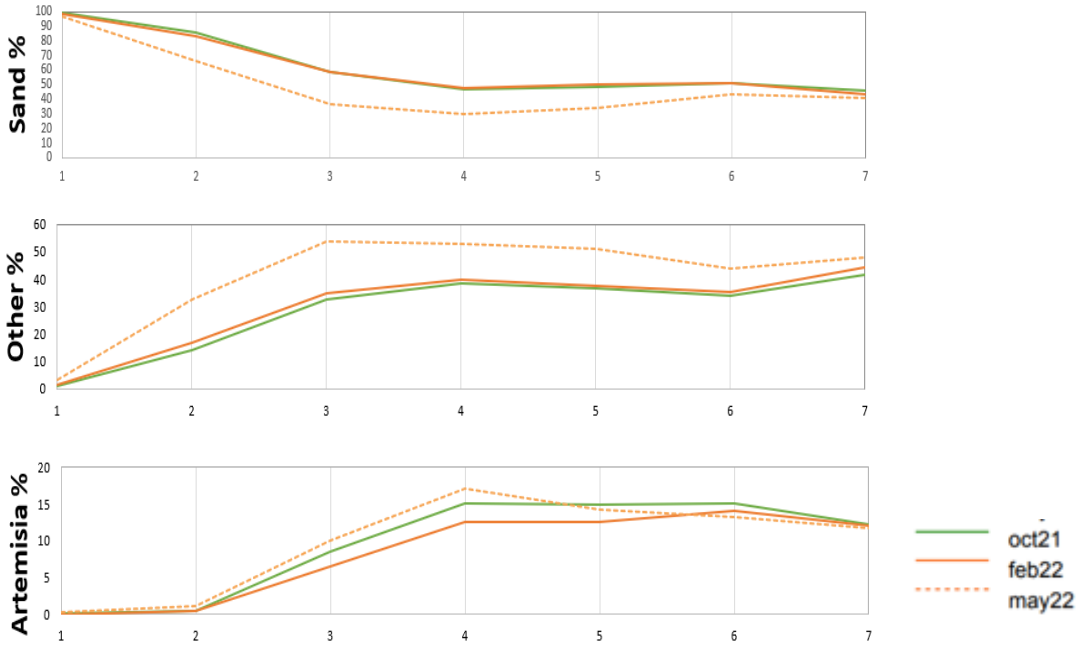

Figure 15: zone 4 cross-shore variation over 7 transects over different seasons and years

5. Discussion

The main challenges in the use of multispectral drone imagery for remote sensing of coastal dune plant species in environments like Ria Formosa, are related with the small size and density of plants and the complexity and heterogeneity of the existing species. Even though the spatial resolution of such imagery can be very high, the spectral resolution offered is low compared with hyperspectral counterparts. This hinders the separation of the spectral signature of distinct plant species and in some cases grouping of species in image classification cannot be avoided.

In order to distinguish dune vegetation in a similar environment in France, Laporte et al. (2020) used an approach to collect ground reference reflectance spectra of each plant species and sand types. Plant species and sand with the lowest mixing percentage where distinguished and used as basis for further RF classification. Ground measurements were performed by deploying a TriOS-RAMSES radiance sensor on a tripod above a 1 x 1 m^2 representative field sites, dominated by one ground cover type.

Prior to any classification attempt or application of any Vegetation Index, the spectral signature of all 21 identified species were evaluated (Appendix A), calculating average values over all plots for every species and every band, which clearly show the high spectral mixing between species in the datasets. In order to simplify the variability in spectral signature, the spatial resolution was decreased (Pu, Landry, & Yu, 2011). For species with distinct signature values were classified separately, and the rest were grouped based on signature similarities over the bands, despite pertaining to different functional types (FTs). On the basis of these results 5 classes, 3 classes and 2 classes were chosen to be tested for the RF classification.

Seasonal variability is reflected in a shift towards higher values in spring compared to the autumn/winter values (fig. 16: Histogram). Perennial species, like *Calystegia* or *Eryngium*, which are mainly consisting out of dead organic material during the winter period seem to disappear almost completely. The NDVI most likely excluded most of the dead material in the winter time. Qi & Wallace (2002) stating that the detection of non-photosynthetic components within multispectral imagery is a challenge due to the fact that the reflectance of such material is similar to that of bare soil. Therefore, a winter disappearance of *Calystegia* or *Eryngium* can be explained by a species transformation into organic dead material. Considering that Eryngium and Calystegia are mainly distributed in the embryo dune, the species could be also disappeared due to winterly overwash.

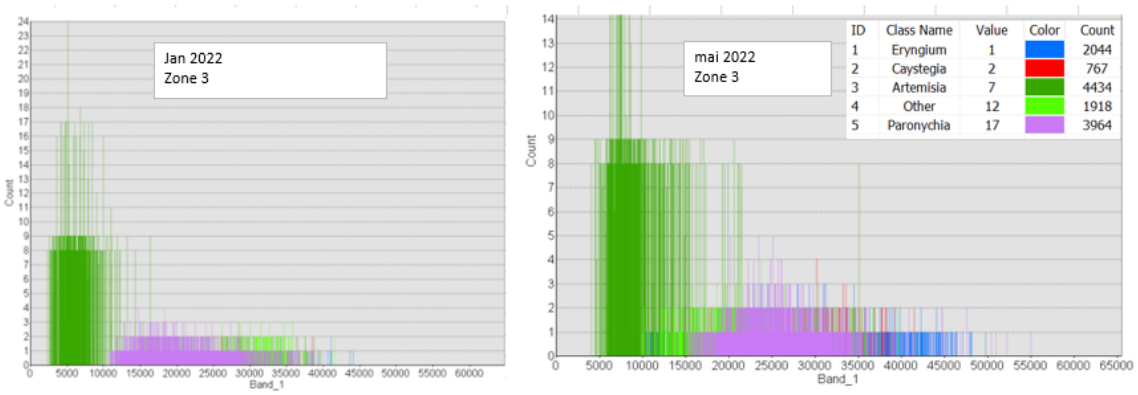

Figure 16: Histogram of January and may in zone 3 for five classes

Accuracies

The overall accuracy of the classification has a significant influence on the reliability of the results and of any deriving ecological conclusions. For the sake of simplicity, the Kappa coefficient will be used for comparisons between study plots whereas the users- and producer accuracy will be used to discuss the implications of different accuracies of the classes that exist within this study. The Kappa coefficient is a widely used metric that describes the overall relationship between the classification and the associated reference data. The use of the Kappa coefficient allows for the direct comparison between different classifications (Congalton & Green, 2008). If Kappa coefficient is below 0.40, the strength of agreement is poor, if the values are between 0.40 and 0.75, it represents an intermediate to good extent of agreement while all values above 0.75 indicate an excellent extent of agreement (Jackson et al., 2019).

The Kappa coefficient was lowest using six classes (zone 2) with a Kappa coefficient of 0.34 in November 2020 and its highest value (0.93) in May 2022 (zone 1), with four classes. Overall, the results are showing higher accuracy values with less classes (see appendix accuracy for zone 2 and zone 3). However, the accuracy results in zone 1 with four classes seem to be better then in zone 3 with just 3 groundcover classes. Considering zone 1 as a very young dune environment which has been just formed in recent years, with less dense vegetation and also less variety of different species, therefore less mixing of different species, resulting in significantly better classification results. The Users accuracy indicates how much of the classified map is actually correctly classified in each class, whereas the Producer accuracy states the correctly classified percentage within each class. The accuracy results of zone 3 is showing low differences between the Users and Producer accuracy, resulting in a very good overall result. The differences between Producer and Users accuracy seem to be higher in zone

2 when classified with six classes, due to mixing between *Other species*, *Eryngium*, *Calystegia* and *Paronychia*. The zone 1, classified in four classes, has good Kappa values (ca. 0.75) and low differences between Producer- and User accuracy in recent campaigns. The campaigns carried out in 2020 show a significantly lower Kappa coefficients (0.60 and 0.63), however with very low success in the classification of *Eryngium* and Other species.

The size of the training data set is a major determinant of classification accuracy. Whereas a a large amount of training data sets is serving a better accuracy, it can be time consuming and therefore challenging. Sample sizes can vary between large training set (n=10.000) and a very small training set (n=40) for a supervised classification (Ramezan et al., 2021). In this study a sample selection of n=15 have been chosen per specie/group in order to be time efficient. However, these rather low sampling size can support a bias in classification, as the training samples may not represent all the species spectral values. Considering the collection of sampling points for the accuracy tests Foody (2009) states that the right amount of sampling point is difficult to define due to extent purpose of the classified plot and also resource and time management. However, the amount of sampling points of n=30 chosen in this study represents a rather small amount comparing to other studies (Laporte et al.,2020; Talavera et al.,2022).

Vegetation cover and community

An overall growth in vegetation coverage can be observed from 2020 to 2021, with a following decline in 2022 in most of the zones and transects. Considering that zones 2, 3 and 4 have very similar dune morphologies and similar zonation, they are comparable in terms of evolution and groundcover changes. In all the three zones (2, 3, 4) there is an increase in vegetation coverage over the analysis period and in the first two sections this could be interpretated as overall seaward progradation of the dune and vegetation. Costas et al. (2021) observed similar cross-shore long-term trends (last decades). An increase in vegetation over the first section can also be interpretated as the fixation and growth of an embryo dune to incipient foredune.

Moving landwards from 30m/40m the more established dune field seem to vary over the years in terms of plant coverage growth with an increase in Plant coverage from 2020 -2021 (*Artemisia* in zone 2, 4; *Other species* in zone 1, 2, 3; *Eryngium* zone 1). Considering extrinsic factors, such as rainfall and air moisture and soil moisture content, which has been low in winter 2019/2020 and also low in 2021/2022 in south Portugal (fig.17), could explain such

developments. However, these trends don't seem to be confirmed in all zones (e.g. *Other species* zone 4 and *Artemisia* zone 3.

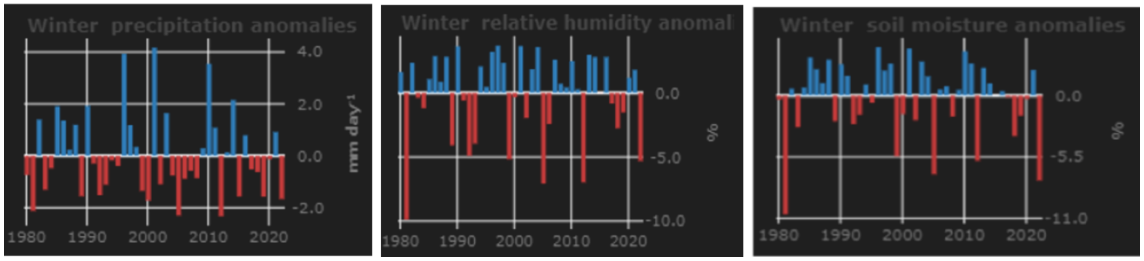

Figure 17: Winter anomalies in Precipitation, humidity and soil moisture in Portugal (Copernicus, 2022)

Ecogeomorphic feedbacks

Previous studies supporting the theory of two topographic states fundamentally governed by the vegetation cover and extrinsic factors. As a biophysical process plant growth is seen as driver in dune recovery and therefore promote dune growth in terms of elevation, while extrinsic factors e.g. storm and sea-level rise tent to control this biological feedback (Stallins, 2005; zinnert et al., 2017; Duran & Moore 2014). Considering this theory and observing rather declining plant vegetation cover in most of the four monitored plots and species towards spring 2022, we could assume a dune decline in elevation as well. However, Costas et al. (2021) explains a decline a limit in vertical growth through low precipitation and low sediment transport preventing the growth of various dune builder plants (e.g *Artemisia*)

6. Conclusion

The Identification of dune species during several fieldtrips via ground truth sampling have been successfully completed. 21 dune vegetation species could be distinguished and related to their dune habitat and grouped into plant functional types. The NDVI could be successfully applied to discriminate sand and dead organic or inorganic matter from live plants. The identification of species via a classification from multispectral drone imagery was rather challenging, because of the similar spectral signature of the species and their high spatial variability. In a preliminary step, individual species and potential species groups were identified, based on the recorded spectral signature. The classification results showed a higher accuracy with less classes, therefore less species/groups could be identified more accurately (and vice versa).

The cross-shore plant zonation over the 4 plots was identified from the classification results. A very low plant coverage over the backshore and embryo dune, with increasing plant coverage landwards, to the dune ridge crest, with related differences in the distribution of plant classes. Due to the challenges in remote sensing at the level of plant species, the spatial variability of zonation was limited to the classes selected (spectrally distinct plant species and groups of mixed dune species).

The acquisition of data through six different fieldtrips over three years in different seasons was used as basis for evaluating the changing dune landcover over time and in all four plots. The tendencies of an advancing vegetation seaward and denser vegetation coverage over seasons/years were identified. Again, due to challenges in classification only certain species/groups could be successfully evaluated in terms of temporal variability.

The UAS data were not able to detect fine-scale community compositional changes and features with any acceptable accuracy. This complexity however, makes the detection and modelling of these plant habitats challenging via UAS imagery based on the methods used in this study.

Appendix A

	Aeonium arboreum	Ammophila arenaria	Anthemis maritima	Artemisia campestris	Cakile maritima	Calystegia soldanella	Carpobrotus acinaciformis	Crucianella maritima	elymus farctus	Eryngium maritimum	Euphorbia paralias	Linaria pedunculata	Lotus creticus	Malcolmia littorea	Medicago marina	Otanthus maritimus	Pancratium maritimum	Paronychia argentea	Pelargonium capitatum	Polygonum maritimum	Silene nicaeensis
Aeonium arboreum	0	9368.08	8151.09	8374.07	4264.12	5511.46	6863.05	7369.81	7945.63	4575.45	4521.85	7468.7	8283.97	7033.86	6209.38	8301.01	5129.9	6914.57	4338.08	8030.03	4201.17
Ammophila arenaria	9368.08	0	1926.47	2066.89	7749.59	4795.04	3894.25	2959.47	2781.94	6360.78	6800.5	2594	1507.11	3988.57	3793.03	3461.1	4735.05	4190.69	7083.83	1693.94	5844.72
Anthemis maritima	8151.09	1926.47	0	445.682	7288.53	4428.98	2128.39	3281.72	3494.53	5827.86	6390.4	2720.12	1034.38	4219.42	3298.67	4164.94	3764.01	4401.87	5340.08	2035.78	4443.47
Artemisia campestris	8374.07	2066.89	445.682	0	7634.08	4804.53	2134.85	3666.01	3860.29	6172.2	6725.92	3134.47	1328.35	4605.8	3672.79	4548.54	4082.49	4783.54	5414.92	2402.18	4656.55
Cakile maritima	4264.12	7749.59	7288.53	7634.08	0	2984.25	6995.79	4937.29	5385.24	1625.45	1113.48	5355.24	6904.71	4115.02	4180.67	5401.42	3778.72	3905.02	6273.04	6141.61	4327.31
Calystegia soldanella	5511.46	4795.04	4428.98	4804.53	2984.25	0	4621.43	2067.65	2631	1653.05	2160.76	2396.33	3968.43	1538.62	1310.08	2853.89	1623.64	1437.65	5325.78	3168.87	3121.05
Carpobrotus acinaciformis	6863.05	3894.25	2128.39	2134.85	6995.79	4621.43	0	4358.8	4763.48	5717.66	6156.26	3911.96	2944.27	5073.16	3797.59	5510.11	3566.26	5161.14	3491.95	3608.33	3361.06
Crucianella maritima	7369.81	2959.47	3281.72	3666.01	4937.29	2067.65	4358.8	0	663.018	3632.8	4053.31	810.854	2554.93	1058.32	1522.88	1373.86	2765.39	1263.62	6328.01	1420.6	4364.33
elymus farctus	7945.63	2781.94	3494.53	3860.29	5385.24	2631	4763.48	663.018	0	4165.19	4501.18	1178.9	2722.22	1399.24	2182.49	1191.34	3426.78	1584.9	6926.14	1523.03	5009.12
Eryngium maritimum	4575.45	6360.78	5827.86	6172.2	1625.45	1653.05	5717.66	3632.8	4165.19	0	1245.63	3961.45	5404.5	2891.22	2665.94	4180.99	2290.43	2748.84	5443.02	4716.57	3229.71
Euphorbia paralias	4521.85	6800.5	6390.4	6725.92	1113.48	2160.76	6156.26	4053.31	4501.18	1245.63	0	4520.71	6007.75	3310.22	3371.55	4678.64	3074.72	3073.51	5834.88	5240.67	3777.17
Linaria pedunculata	7468.7	2594	2720.12	3134.47	5355.24	2396.33	3911.96	810.854	1178.9	3961.45	4520.71	0	2015.74	1658.93	1511.47	1615.25	2701.16	1901.86	6062.62	972.823	4234.71
Lotus creticus	8283.97	1507.11	1034.38	1328.35	6904.71	3968.43	2944.27	2554.93	2722.22	5404.5	6007.75	2015.74	0	3484.64	2770.75	3284.56	3515.47	3694.75	5855.41	1209.38	4545.62
Malcolmia littorea	7033.86	3988.57	4219.42	4605.8	4115.02	1538.62	5073.16	1058.32	1399.24	2891.22	3310.22	1658.93	3484.64	0	1563.16	1411.67	2677.17	321.949	6533.69	2415.35	4356.25
Medicago marina	6209.38	3793.03	3298.67	3672.79	4180.67	1310.08	3797.59	1522.88	2182.49	2665.94	3371.55	1511.47	2770.75	1563.16	0	2446.67	1288.03	1670.97	5098.17	2138.43	2973.72
Otanthus maritimus	8301.01	3461.1	4164.94	4548.54	5401.42	2853.89	5510.11	1373.86	1191.34	4180.99	4678.64	1615.25	3284.56	1411.67	2446.67	0	3705.21	1664.04	7463.81	2170.16	5403.36
Pancratium maritimum	5129.9	4735.05	3764.01	4082.49	3778.72	1623.64	3566.26	2765.39	3426.78	2290.43	3074.72	2701.16	3515.47	2677.17	1288.03	3705.21	0	2690.87	3997.1	3208.82	1742.88
Paronychia argentea	6914.57	4190.69	4401.87	4783.54	3905.02	1437.65	5161.14	1263.62	1584.9	2748.84	3073.51	1901.86	3694.75	321.949	1670.97	1664.04	2690.87	0	6526.21	2635.82	4326.82
Pelargonium capitatum	4338.08	7083.83	5340.08	5414.92	6273.04	5325.78	3491.95	6328.01	6926.14	5443.02	5834.88	6062.62	5855.41	6533.69	5098.17	7463.81	3997.1	6526.21	0	6207.03	2409.04
Polygonum maritimum	8030.03	1693.94	2035.78	2402.18	6141.61	3168.87	3608.33	1420.6	1523.03	4716.57	5240.67	972.823	1209.38	2415.35	2138.43	2170.16	3208.82	2635.82	6207.03	0	4568.61
Silene nicaeensis	4201.17	5844.72	4443.47	4656.55	4327.31	3121.05	3361.06	4364.33	5009.12	3229.71	3777.17	4234.71	4545.62	4356.25	2973.72	5403.36	1742.88	4326.82	2409.04	4568.61	0

Figure 18: differences in signals

grouping threshold	1200																				
	Aeonium arboreum	Ammophila arenaria	Anthemis maritima	Artemisia campestris	Cakile maritima	Calystegia soldanella	Carpobrotus acinaciformis	Crucianella maritima	elymus farctus	Eryngium maritimum	Euphorbia paralias	Linaria pedunculata	Lotus creticus	Malcolmia littorea	Medicago marina	Otanthus maritimus	Pancratium maritimum	Paronychia argentea	Pelargonium capitatum	Polygonum maritimum	Silene nicaeensis
Aeonium arboreum	yes	no	no	no	no	no	no	no	no	no	no	no	no	no	no	no	no	no	no	no	no
Ammophila arenaria	no	yes	no	no	no	no	no	no	no	no	no	no	no	no	no	no	no	no	no	no	no
Anthemis maritima	no	no	yes	yes	no	no	no	no	no	no	no	no	yes	no	no	no	no	no	no	no	no
Artemisia campestris	no	no	yes	yes	no	no	no	no	no	no	no	no	no	no	no	no	no	no	no	no	no
Cakile maritima	no	no	no	no	yes	no	no	no	no	no	yes	no	no	no	no	no	no	no	no	no	no
Calystegia soldanella	no	no	no	no	no	yes	no	no	no	no	no	no	no	no	no	no	no	no	no	no	no
Carpobrotus acinaciformis	no	no	no	no	no	no	yes	no	no	no	no	no	no	no	no	no	no	no	no	no	no
Crucianella maritima	no	no	no	no	no	no	no	yes	yes	no	no	yes	no	yes	no	no	no	no	no	no	no
elymus farctus	no	no	no	no	no	no	no	yes	yes	no	no	yes	no	no	no	yes	no	no	no	no	no
Eryngium maritimum	no	no	no	no	no	no	no	no	no	yes	no	no	no	no	no	no	no	no	no	no	no
Euphorbia paralias	no	no	no	no	yes	no	no	no	no	no	yes	no	no	no	no	no	no	no	no	no	no
Linaria pedunculata	no	no	no	no	no	no	no	yes	yes	no	no	yes	no	no	no	no	no	no	no	yes	no
Lotus creticus	no	no	yes	no	no	no	no	no	no	no	no	no	yes	no	no	no	no	no	no	no	no
Malcolmia littorea	no	no	no	no	no	no	no	yes	no	no	no	no	no	yes	no	no	no	yes	no	no	no
Medicago marina	no	no	no	no	no	no	no	no	no	no	no	no	no	no	yes	no	no	no	no	no	no
Otanthus maritimus	no	no	no	no	no	no	no	no	yes	no	no	no	no	no	no	yes	no	no	no	no	no
Pancratium maritimum	no	no	no	no	no	no	no	no	no	no	no	no	no	no	no	no	yes	no	no	no	no
Paronychia argentea	no	no	no	no	no	no	no	no	no	no	no	no	no	yes	no	no	no	yes	no	no	no
Pelargonium capitatum	no	no	no	no	no	no	no	no	no	no	no	no	no	no	no	no	no	no	yes	no	no
Polygonum maritimum	no	no	no	no	no	no	no	no	no	no	no	yes	no	no	no	no	no	no	no	yes	no
Silene nicaeensis	no	no	no	no	no	no	no	no	no	no	no	no	no	no	no	no	no	no	no	no	yes

Figure 19: similarities in signals

GROUPS				450	560	650	730	840
A	Aeonium arboreum			17061	32815	19148	52242	55442
B	Ammophila arenaria			13238.25	14421.5	12987.25	21505.5	26143.5
C	Anthemis maritima	Artemisia campestris	Lotus creticus	12614.58333	13631.75	9473.167	25372	33123.42
D	Cakile maritima	Euphorbia paralias		27362.5	29248.17	28153.17	40895.17	43340.83
E	Calystegia soldanella			23920.33333	24390.33	21008	34483.67	37482
F	Carpobrotus acinaciformis			8441	12812	8394	34961	38447
G	Crucianella maritima			21609.8	21274.2	19370.2	27715.8	30898.4
H	Eryngium maritimum			27254.75	27577.25	23071	36896.25	43561.75
I	Medicago marina			22680.5	20897.17	17012.33	30853.5	37323.83
J	elymus farctus	Otanthus maritimus		24169.08333	21776.88	19694.29	25426.96	28057.38
K	Pancratium maritimum			21888.25	20806.75	15997	34654.25	42360
L	Malcolmia littorea	Paronychia argentea		25460.06667	23001.1	22425.8	29411.73	32712.93
M	Pelargonium capitatum			10749	16935	8320	45427	51599
N	Linaria pedunculata	Polygonum maritimum		16066.75	18590.75	11892.75	36672	41145
O	Silene nicaeensis			18577.75	18520.25	14324	39861.5	47822.5

Figure 20: grouping of signals

Table 10:accuracy of plots one for the different dates

date	Kappa	overall Acuracy	Comission	Omission	Users Acuracy	Producer Acuracy	landcover
21.05.2020	0.60	0.70	11.76	0.00	88.24	100.00	Sand
			3.45	6.67	96.55	93.33	Otanthus
			100.00	100.00	0.00	0.00	Eryngium
			52.73	13.33	47.27	86.67	Other
26.11.2020	0.63	0.73	9.09	0.00	90.91	100.00	Sand
			19.44	3.33	80.56	96.67	Otanthus
			33.33	86.67	66.67	13.33	Eryngium
			46.67	20.00	53.33	80.00	Other

07.05.2021	0.90	0.93	3.23	0.00	96.77	100.00	Sand
			3.45	6.67	96.55	93.33	Otanthus
			10.00	10.00	90.00	90.00	Eryngium
			13.33	13.33	86.67	86.67	Other
13.10.2021	0.91	0.93	3.23	0.00	96.77	100.00	Sand
			9.09	0.00	90.91	100.00	Otanthus
			6.90	10.00	93.10	90.00	Eryngium
			7.41	16.67	92.59	83.33	Other
03.02.2022	0.92	0.94	3.23	0.00	96.77	100.00	Sand
			3.33	3.33	96.67	96.67	Otanthus
			6.90	10.00	93.10	90.00	Eryngium
			10.00	10.00	90.00	90.00	Other
18.05.2022	0.93	0.95	3.23	0.00	96.77	100.00	Sand
			3.23	0.00	96.77	100.00	Otanthus
			6.67	6.67	93.33	93.33	Eryngium
			7.14	13.33	92.86	86.67	Other

Table 1: plot2 accuracy

Table 11: Accuracy for plot 2 for the different dates

date	Kappa	overall Acuracy	Comission	Omission	Users Acuracy	Producer Acuracy	landcover
21.05.2020	0.37	0.48	55.56	20.00	44.44	80.00	sand
			51.85	56.67	48.15	43.33	eryngium
			54.55	83.33	45.45	16.67	calystegia
			31.58	13.33	68.42	86.67	artemesia
			74.07	76.67	25.93	23.33	Other
			52.17	63.33	47.83	36.67	paronychia
26.11.2020	0.34	0.44	52.73	13.33	47.27	86.67	sand
			58.82	74.07	41.18	23.33	eryngium
			0.00	100.00	0.00	0.00	calystegia
			32.43	16.67	67.57	83.33	artemesia
			75.86	75.00	24.14	23.33	Other
			51.85	56.67	48.15	43.33	paronychia
07.05.2021	0.40	0.50	41.30	10.00	58.70	90.00	sand
			57.58	53.33	42.42	46.67	eryngium
			25.00	90.00	75.00	10.00	calystegia
			26.47	16.67	73.53	83.33	artemesia
			74.42	63.33	25.58	36.67	Other
			50.00	66.67	50.00	33.33	paronychia
13.10.2021	0.42	0.52	48.28	0.00	51.72	100.00	sand
			65.52	66.67	34.48	33.33	eryngium
			0.00	96.67	100.00	3.33	calystegia
			27.03	10.00	72.97	90.00	artemesia
			60.53	50.00	39.47	50.00	Other

			41.18	66.67	58.82	33.33	paronychia
03.02.2022	0.43	0.53	57.14	0.00	42.86	100.00	sand
			91.67	93.33	8.33	6.67	eryngium
			0.00	100.00	0.00	0.00	calystegia
			26.83	0.00	73.17	100.00	artemesia
			25.93	33.33	74.07	66.67	Other
			27.78	56.67	72.22	43.33	paronychia
18.05.2022	0.41	0.51	55.56	20.00	44.44	80.00	sand
			43.48	56.67	56.52	43.33	eryngium
			37.50	66.67	62.50	33.33	calystegia
			31.58	13.33	68.42	86.67	artemesia
			73.08	76.67	26.92	23.33	Other
			52.17	63.33	47.83	36.67	paronychia

Table 12: Accuracy for plot 3 for the different dates

date	Kappa	overall	Comission	Omission	User	Producers	landcover
21.05.2020	0.80	0.87	12.12	3.33	87.88	96.67	Sand
			11.11	20.00	88.89	80.00	Artemísia
			16.67	16.67	83.33	83.33	other
26.11.2020	0.82	0.88	11.76	0.00	88.24	100.00	Sand
			13.79	16.67	86.21	83.33	Artemísia
			11.11	20.00	88.89	80.00	other
07.05.2021	0.78	0.86	15.63	10.00	84.38	90.00	Sand
			17.65	6.67	82.35	93.33	Artemísia
			8.33	26.67	91.67	73.33	other
13.10.2021	0.83	0.89	12.12	3.33	87.88	96.67	Sand
			15.63	10.00	84.38	90.00	Artemísia
			4.00	20.00	96.00	80.00	other
03.02.2022	0.78	0.86	19.44	3.33	80.56	96.67	Sand
			13.04	33.33	86.96	66.67	Artemísia
			9.68	6.67	90.32	93.33	other
18.05.2022	0.80	0.87	12.50	6.67	87.50	93.33	Sand
			14.81	23.33	85.19	76.67	Artemísia
			12.90	10.00	87.10	90.00	other

References

Adam, E., Mutanga, O., Rugege, D. Multispectral and hyperspectral remote sensing for identification and mapping of wetland vegetation: A review. Wetlands Ecol. Manag. 2010, 18, 281–296.

Anderson, K., & Gaston, K. J. (2013). Lightweight unmanned aerial vehicles will revolutionize spatial ecology. Frontiers in Ecology and the Environment, 11(3), 138-146. doi:10.1890/120150

Asrar G, Fuch M, Kanemasu ET, et al. (1984) Estimating absorbed photosynthetic radiation and leaf produce index from spectral reflectance in wheat. Agron J 76:300–6.

Bemis, S.P., Micklethwaite, S., Turner, D., James, M.R., Akciz, S., Thiele, S.T., Ali, H. Ground-based and UAV-based photogrammetry: A multi-scale, high-resolution mapping tool for structural geology and paleoseismology. J. Struct. Geol. 2014, 69, 163–178.

Brodie, Katherine, Conery, Ian, Cohn, Nicholas, Spore, Nicholas, Palmsten, Margaret (2019). Spatial Variability of Coastal Foredune Evolution, Part A: Timescales of Months to Years. Journal of Marine Science and Engineering, 7(5), 124–. doi:10.3390/jmse7050124

Buckley, Ralf (1987). The effect of sparse vegetation on the transport of dune sand by wind. , 325(6103), 426–428. doi:10.1038/325426a0

Carley J T & Cox R J (2017). NSW Office of Environment and Heritage's Coastal Processes and Responses Node - Technical Report. Guidelines for Sand Nourishment. University of New South Wales Water Research Laboratory. 5:1-57.

Ciccarelli, D., Garbari F. & Bedini G. (2009): Plant Functional Types in Tuscan coastal dunes. — Fl. Medit. 19: 199-206. 2009. — ISSN 1120-4052.

Ciccarelli, D., & Bona, C. (2021). Exploring the Functional Strategies Adopted by Coastal Plants Along an Ecological Gradient Using Morpho-functional Traits. Estuaries and Coasts. doi:10.1007/s12237-021-00945-y

Chen, Yongxin, Hezi Yizhaq, Joseph A. Mason, Xueliang Zhang, Zhiwei Xu,(2021): Dune bistability identified by remote sensing in a semi-arid dune field of northern China, Aeolian Research, Volume 53,100751, ISSN 1875-9637,https://doi.org/10.1016/j.aeolia.2021.100751

Christopher A. Ramezan;Timothy A. Warner;Aaron E. Maxwell;Bradley S. Price; (2021). Effects of Training Set Size on Supervised Machine-Learning Land-Cover Classification of Large-Area High-Resolution Remotely Sensed Data . Remote Sensing, (), – . doi:10.3390/rs13030368

Costas, Susana, de Sousa, Luisa Bon, Kombiadou, Katerina, Ferreira, Óscar, Plomaritis, Theocharis A. (2020). *Exploring foredune growth capacity in a coarse sandy beach. Geomorphology, 371(), 107435–.* doi:10.1016/j.geomorph.2020.107435

Costas, Susana, Gallego-Ferandez, Juan B., Bon de Sousa, Luisa, Kombiadou, Katerina (under review). Ecogeomorphic adaptation of a coastal dune in Southern Portugal regulated by extrinsic factors --Manuscript Draft-- Research Paper.

Correll, Maureen D., Hantson, Wouter, Hodgman, Thomas P., Cline, Brittany B., Elphick, Chris S., Gregory Shriver, W., Tymkiw, Elizabeth L., Olsen, Brian J. (2018). *Fine-Scale Mapping*

of Coastal Plant Communities in the Northeastern USA. Wetlands, (), –. doi:10.1007/s13157-018-1028-3

Davies, J.L., 1980. Geographical Variation in Coastal Development. Longman, London, p. 204.

De Giglio, Michaela, Greggio, Nicolas, Goffo, Floriano, Merloni, Nicola, Dubbini, Marco, Barbarella, Maurizio (2019). Comparison of Pixel- and Object-Based Classification Methods of Unmanned Aerial Vehicle Data Applied to Coastal Dune Vegetation Communities: Casal Borsetti Case Study. Remote Sensing, 11(12), 1416–. doi:10.3390/rs11121416

Du, Jianhui, Hesp, Patrick A. (2020). Salt Spray Distribution and Its Impact on Vegetation Zonation on Coastal Dunes: a Review. Estuaries and Coasts, (), –. doi:10.1007/s12237-020-00820-2

Duran, O., Moore, L. J. (2013). Vegetation controls on the maximum size of coastal dunes. Proceedings of the National Academy of Sciences, 110(43), 17217–17222. doi:10.1073/pnas.1307580110

Durán Vinent, Orencio, Moore, Laura J. (2014). Barrier island bistability induced by biophysical interactions. Nature Climate Change, 5(2), 158–162. doi:10.1038/nclimate2474

Óscar Ferreira, Tiago Garcia, Ana Matias, Rui Taborda, J. Alveirinho Dias,(2006). An integrated method for the determination of set-back lines for coastal erosion hazards on sandy shores, Continental Shelf Research, Volume 26, Issue 9, ,Pages 1030-1044

Feng, Quanlong, Liu, Jiantao, Gong, Jianhua (2015). *UAV Remote Sensing for Urban Vegetation Mapping Using Random Forest and Texture Analysis. Remote Sensing, 7(1), 1074–1094.* doi:10.3390/rs70101074

Foody, G. M., & Mathur, A. (2004). Toward intelligent training of supervised image classifications: directing training data acquisition for SVM classification. Remote Sensing of Environment, 93(1-2), 107-117.

Foody. (1996). Fuzzy modelling of vegetation from remotely sensed imagery. Ecological Modelling, 85(1), 3-12. doi:https://doi.org/10.1016/0304-3800(95)00012-7

Foody. (1996). (2009). *Sample size determination for image classification accuracy assessment and comparison. International Journal of Remote Sensing, 30(20), 5273–5291.* doi:10.1080/01431160903130937

Ford K, Harris JR, Shives R, Carson J, and Buckle J (2008b) Remote predictive mapping 2. Gamma ray spectrometry: A tool for mapping Canada's north. *Geoscience Canada* 35: 109–126.

Galio KP, Daughtry CST, Bauer ME (1985) Spectral estimation of absorbed photosynthetically active radiation in corn canopies. Agron J 78:752–6.

García-Mora M. Rosario, Juan B. Gallego-Fernández and Francisco García-Novo (1999). Plant Functional Types in Coastal Foredunes in Relation to Environmental Stress and Disturbance. Journal of Vegetation Science, 10(1), 27–34. doi:10.2307/3237157

Gini, R., Passoni, D., Pinto, L., Sona, G. (2012). Aerial images from an UAV system: 3d modeling and tree species classification in a park area. Int. Arch. Photogram. Remote Sens. Spat. Inf. Sci., 39, 361–366.

Hesp, Patrick A. (1989). A review of biological and geomorphological processes involved in the initiation and development of incipient foredunes. Proceedings of the Royal Society of

Edinburgh. Section B. Biological Sciences, 96(), 181–201. doi:10.1017/s0269727000010927

Hesp P. (2002). Foredunes and blowouts: initiation, geomorphology and dynamics. , 48(1-3), 0–268. doi:10.1016/s0169-555x(02)00184-8

Houser, C. (2013). Treatise on Geomorphology || 10.10 Beach and Dune Interaction. , (), 267–288. doi:10.1016/B978-0-12-374739-6.00283-9

Huang, C., Davis, L. S., & Townshend, J. R. G. (2002). An assessment of support vector machines for land cover classification. International Journal of Remote Sensing, 23(4), 725-749. doi:10.1080/01431160110040323

Jackson, Derek W.T., Costas, Susana, González-Villanueva, Rita, Cooper, Andrew (2019). A global 'greening' of coastal dunes: An integrated consequence of climate change?. Global and Planetary Change, 182(), 103026–. doi:10.1016103026

Kaneko, K., Nohara, S. Review of effective vegetation mapping using the UAV (Unmanned Aerial Vehicle) method. Int. J. Geogr. Inf. Sci. 2014, 6, 733–742.

Langley, S. K., Cheshire, H. M., & Humes, K. S. (2001). A comparison of single date and multitemporal satellite image classifications in a semi-arid grassland. Journal of Arid Environments, 49(2), 401-411.

Laporte-Fauret, Quentin, Lubac, Bertrand, Castelle, Bruno, Michalet, Richard, Marieu, Vincent, Bombrun, Lionel, Launeau, Patrick, Giraud, Manuel, Normandin, Cassandra, Rosebery, David (2020). *Classification of Atlantic Coastal Sand Dune Vegetation Using In Situ, UAV, and Airborne Hyperspectral Data. Remote Sensing, 12(14), 2222–.* doi:10.3390/rs12142222

Lawley, V., Lewis, M., Clarke, K., Ostendorf, B. Site-based and remote sensing methods for monitoring indicators of vegetation condition: An Australian review. Ecol. Indic. 2016, 60, 1273–1283.

Lu, D., Weng, Q. (2007). A survey of image classification methods and techniques for improving classification performance. , 28(5), 823–870. doi:10.1080/01431160600746456

Manfreda, S., McCabe, M. E., Miller, P. E., Lucas, R., Madrigal, V. P., Mallinis, G., . . . Toth, B. (2018). On the Use of Unmanned Aerial Systems for Environmental Monitoring. Remote Sensing, 10(4). doi:10.3390/rs10040641

Maun, M. A. (2009). The Biology of Coastal Sand Dunes. New York: Oxford University Press

Martins, Mónica C. , Carlos S. Neto, José C. Costa (2013). The meaning of mainland Portugal beaches and dunes' psammophilic plant communities: a contribution to tourism management and nature conservation. , 17(3), 279–299. doi:10.1007/s11852-013-0232-9

Marzialetti, Flavio, Giulio, Silvia, Malavasi, Marco, Sperandii, Marta Gaia, Acosta, Alicia Teresa Rosario, Carranza, Maria Laura (2019). *Capturing Coastal Dune Natural Vegetation Types Using a Phenology-Based Mapping Approach: The Potential of Sentinel-2. Remote Sensing, 11(12), 1506–.* doi:10.3390/rs11121506

Motohka, Takeshi, Nasahara, Kenlo Nishida, Oguma, Hiroyuki, Tsuchida, Satoshi (2010). *Applicability of Green-Red Vegetation Index for Remote Sensing of Vegetation Phenology. Remote Sensing, 2(10), 2369–2387.* doi:10.3390/rs2102369

Navulur K (2006) Multispectral Image Analysis Using the Object-Oriented Paradigm. New York: Taylor and Francis,

Nevalainen, O., Hakala, T., Suomalainen, J., Mäkipää, R., Peltoniemi, M., Krooks, A., & Kaasalainen, S. (2014). Fast and nondestructive method for leaf level chlorophyll estimation using hyperspectral LiDAR. Agricultural and Forest Meteorology, 198-199, 250-258. doi:https://doi.org/10.1016/j.agrformet.2014.08.018

Otukei, J. R., & Blaschke, T. (2010). Land cover change assessment using decision trees, support vector machines and maximum likelihood classification algorithms. International Journal of Applied Earth Observation and Geoinformation, 12, S27-S31. doi:https://doi.org/10.1016/j.jag.2009.11.002

Pajares, G. Overview and current status of remote sensing applications based on unmanned aerial vehicles (UAVs). Photogr. Eng. Remote Sens. 2015, 81, 281–329.

Pliatsika, Dimitra Alkisti. (2018). Aeolian sediment transport potentials and dune evolution in Ancão Peninsula (Ria Formosa), Portugal Work performed under the supervision of.

Proença, Bárbara, Frappart, Frédéric, Lubac, Bertrand, Marieu, Vincent, Ygorra, Bertrand, Bombrun, Lionel, Michalet, Richard, Sottolichio, Aldo (2019). *Potential of High-Resolution Pléiades Imagery to Monitor Salt Marsh Evolution After Spartina Invasion. Remote Sensing, 11(8), 968–.* doi:10.3390/rs11080968

Pu, R., Landry, S., & Yu, Q. (2011). Object-based urban detailed land cover classification with high spatial resolution IKONOS imagery. International Journal of Remote Sensing, 32(12), 3285- 3308. doi:10.1080/01431161003745657

Pye, K. (1983). Coastal dunes. Progress in Physical Geography, 7(4), 531–557. doi:10.1177/030913338300700403

Pye, K., & Tsoar, H. (. (2009). Aeolian Sand and Sand Dunes. Leipzig: Springer-Verlag BerlinHeidelberg.

Qi, X.K., Wang, K.L., Zhang, C.H. (2013): Effectiveness of ecological restoration projects in a karst region of southwest China assessed using vegetation succession mapping. Ecol. Eng. 2013, 54, 245–253.

Kozhoridze, G., Orlovsky, N., Orlovsky, L., Blumberg, D.G., Golan-Goldhirsh, A. Remote sensing models of structure-related biochemicals and pigments for classification of trees. Remote Sens. Environ. 2016, 186, 184–195.

Renaud, Fabrice G., Sudmeier-Rieux, Karen, Estrella, Marisol, Nehren, Udo (2016). [Advances in Natural and Technological Hazards Research] Ecosystem-Based Disaster Risk Reduction and Adaptation in Practice Volume 42 || . , 10.1007/978-3-319-43633-3(), –. doi:10.1007/978-3-319-43633-3

Richardson A. J. and Weigand C. (1977): "Distinguishing vegetation from soil background information," Photogrammetric Engineering and Remote Sensing, p. 43,

Seabloom, Eric W., Ruggiero, Peter, Hacker, Sally D., Mull, Jeremy, Zarnetske, Phoebe (2013). Invasive grasses, climate change, and exposure to storm-wave overtopping in coastal dune ecosystems. Global Change Biology, 19(3), 824–832. doi:10.1111/gcb.12078

Singh, K. K., & Frazier, A. E. (2018). A meta-analysis and review of unmanned aircraft system (UAS) imagery for terrestrial applications. *International Journal of Remote Sensing*, *39*(15-16), 5078-5098.

Suo, , McGovern, , Gilmer, (2019). *Coastal Dune Vegetation Mapping Using a Multispectral Sensor Mounted on an UAS. Remote Sensing, 11(15), 1814–.* doi:10.3390/rs11151814

Suo, , McGovern, , Gilmer, (2019). *Coastal Dune Vegetation Mapping Using a Multispectral Sensor Mounted on an UAS. Remote Sensing, 11(15), 1814–.* doi:10.3390/rs11151814

Talavera, Susana Costas, Óscar Ferreira (2022), A new index to assess the state of dune vegetation derived from true colour images, Ecological Indicators, Volume 137, 2022, 108770, ISSN 1470-160X, https://doi.org/10.1016/j.ecolind.2022.108770.

Turner, W., Spector, S., Gardiner, N., Fladeland, M., Sterling, E., & Steininger, M. (2003). Remote sensing for biodiversity science and conservation. Trends in Ecology & Evolution, 18(6), 306- 314. doi:10.1016/s0169-5347(03)00070-3

Turner, I.L., Harley, M.D., Drummond, C.D. UAVs for coastal surveying. Coast. Eng. 2016, 114, 19–24

Underwood, E. C., Ustin, S. L., & Ramirez, C. M. (2007). A comparison of spatial and spectral image resolution for mapping invasive plants in coastal California. Environmental Management, 39(1), 63-83. doi:10.1007/s00267-005-0228-9

Valentini, Emiliana, Taramelli, Andrea, Cappucci, Sergio, Filipponi, Federico, Nguyen Xuan, Alessandra (2020). Exploring the Dunes: The Correlations between Vegetation Cover Pattern and Morphology for Sediment Retention Assessment Using Airborne Multisensor Acquisition. Remote Sensing, 12(8), 1229–. doi:10.3390/rs12081229

Venturi, S., Di Francesco, S., Materazzi, F., Manciola, P. Unmanned aerial vehicles and Geographical Information System integrated analysis of vegetation in Trasimeno Lake, Italy. Lakes Reserv. Res. Manag. 2016, 21, 5–19.

Verbesselt, J., Hyndman, R., Newnham, G., Culvenor, D. Detecting trend and seasonal changes in satellite image time series. Remote Sens. Environ. 2010, 114, 106–115.

Walters, Michele, Scholes, Robert J. (2017). *The GEO Handbook on Biodiversity Observation Networks || Remote Sensing for Biodiversity. , 10.1007/978-3-319-27288-7(Chapter 8), 187–210.* doi:10.1007/978-3-319-27288-7_8

Weier, J. & Herring, D (2000). Measuring vegetation (NDVI & EVI). https://earthobservatory.nasa. gov/Features/MeasuringVegetation/. Accessed december 4, 2021.

Wiedemann, A. M., & Pickart, A. J. (2008). *Temperate Zone Coastal Dunes. Coastal Dunes, 53–65.* doi:10.1007/978-3-540-74002-5_4

Xie, Y., Sha, Z., Yu, M. (2008). Remote sensing imagery in vegetation mapping: a review. , 1(1), 9–23. doi:10.1093/jpe/rtm005

Xu, Dandan, Guo, Xulin, Li, Zhaoqin, Yang, Xiaohui, Yin, Han (2014). Measuring the dead component of mixed grassland with Landsat imagery. Remote Sensing of Environment, 142(), 33–43. doi:10.1016/j.rse.2013.11.017

Zarnetske, P. L., Ruggiero, P., Seabloom, E. W., Hacker, S. D. (2015). Coastal foredune evolution: the relative influence of vegetation and sand supply in the US Pacific Northwest. Journal of The Royal Society Interface, 12(106), 20150017–20150017. doi:10.1098/rsif.2015.0017

Zhang W. (2016) Barrier Island. In: Kennish M.J. (eds) Encyclopedia of Estuaries. Encyclopedia of Earth Sciences Series. Springer, Dordrecht. https://doi.org/10.1007/978-94-017-8801-4_124

Zinnert, Julie C., Stallins, J. Anthony, Brantley, Steven T., Young, Donald R. (2017). Crossing Scales: The Complexity of Barrier-Island Processes for Predicting Future Change. BioScience, 67(1), 39–52. doi:10.1093/biosci/biw154

Online:

Copernicus (2022): https://cds.climate.copernicus.eu/cdsapp#!/software/app-c3s-monthly-climate-bulletin-explorer